UNIVERSIDADE DE LISBOA
FACULDADE DE CIÊNCIAS
DEPARTAMENTO DE BIOLOGIA VEGETAL

Impact of early centrosome deregulation in malignant transformation

Inês Simões Gomes

Mestrado em Biologia Molecular e Genética

Dissertação orientada por:
Prof. Doutora Carla A. M. Lopes

2021

ACKNOWLEDGMENTS

Está a chegar ao fim o que para mim foi um dos melhores anos do meu percurso académico. O ano em que finalmente pude pôr em prática e aplicar tudo o que aprendi. Apesar de ter sido um ano com condições atípicas e bastante desafiante, posso afirmar que foi o melhor ano do meu percurso enquanto estudante. Foi um ano trabalhoso, cheio de desafios, mas não foi um percurso que percorri sozinha e por isso tenho muitas pessoas a quem agradecer.

Quero começar por agradecer à minha orientadora, Carla Lopes. Agradeço imenso por me ter dado a oportunidade de fazer parte do grupo de estudos do esófago de Barrett. Quero agradecer por tudo o que me ensinou e por todo o apoio neste meu percurso e por ter puxado pelo meu espirito crítico e por ter deixado que este trabalho se tornasse meu. Agradeço todo o apoio, não poderia pedir melhor orientação, e o meu maior agradecimento vai para ela, sem dúvida.

Gostava de agradecer ao serviço de anatomia patológica do IPO de Lisboa, por me terem recebido tão bem e por me fazerem sentir em casa.

Gostaria também de agradecer ao grupo "Cell Cycle Regulation" do Instituto Gulbenkian Ciência, por me terem recebido de braços abertos nas suas meetings e também em algum trabalho de laboratório. Obrigada por me terem proporcionado um ótimo ambiente científico. Gostava de agradecer a todos os membros, com uma atenção particular para a Catarina Peneda, Miguel Pereira e Marco Louro, pelas reuniões semanais onde pude partilhar todas as minhas conquistas e frustrações deste ano e pelos momentos de convívio. Obrigada pelas discussões interessantes e por me ajudarem a desenvolver este projeto.

Agradeço aos meus professores, quer da licenciatura quer do mestrado, por me terem dado as bases, e muitas dores de cabeça também mas que valeram a pena neste meu percurso para futura bióloga.

Agradeço também a todos os meus amigos próximos que me acompanharam, com um miminho especial para estas 4 grandes amigas que a vida me apresentou. Alexandra, agradeço profundamente a tua amizade. Obrigada por seres a minha amiga de todas as horas, por levares com os meus stresses e ansiedades mas também por me ouvires com entusiasmo a falar sobre o meu trabalho e as minhas experiências. Obrigada por estares sempre presente. Andreia, obrigada por seres o meu amparo e por me teres deixado ser o teu para a tua tese também. Rita e Mafalda, obrigada pelas conversas de apoio. Este agradecimento especial é para vocês, obrigada pelo apoio incondicional.

Ao meu namorado, por levar comigo 24h por dia, quer quando as coisas corriam mal, quer quando corriam bem. Obrigada por aturares o meu entusiasmo e as minhas conversas longas sobre as experiências que estava a fazer. Obrigada pela ajuda, pelo apoio e por acreditares em mim e me motivares.

Por fim, o agradecimento mais importante. Obrigada aos meus pais, por me terem dado oportunidade e por terem feito tudo para eu poder estar na faculdade e a estudar para ser o que quero ser. Obrigada por acreditarem em mim e no meu potencial e estarem sempre aqui a ouvir-me falar de centríolos sem perceberem sequer o que são. Esta tese é para vocês.

ABSTRACT

Centrosome amplification (CA) is a hallmark of human cancers and is therefore a potential feature to explore for prognosis and therapy. However, the poor understanding of its origin and impact has limited its use in the clinic. Here, we used Barrett's esophagus (BE) tumorigenesis as a human cancer model to test if CA has a contributory role in tumorigenesis and progression.

Barrett's esophagus is a premalignant condition and its neoplastic progression is a process with well-characterized and defined steps that go from metaplasia (premalignant condition - BE) to dysplasia (low- or high-grade intraepithelial neoplasia), adenocarcinoma (invasive neoplasia) and metastasis. Given that CA arises in BE metaplasia and that its incidence significantly increases from metaplasia to dysplasia, we posed the hypothesis that CA may play an important role in the acquisition of malignant properties. If this hypothesis is correct, then an increase of CA in metaplasia and/or a decrease of CA in dysplasia would be sufficient to respectively promote or reduce malignant properties such as invasiveness potential.

To test these hypotheses, we first tested two different methods to reduce the CA levels in dysplasia cells: depletion of important molecules in the centrosome duplication cycle - PLK4, SAS6 and STIL - by siRNA, and inhibition of PLK4 activity using the specific chemical inhibitor centrinone-B. We then assessed changes in migration and invasive potential using 2D migration and invasion assays and 3D cell cultures. Both strategies were effective in reducing CA in dysplasia cells but as the treatment with the inhibitor acts directly on the protein's activity level, its effects were more quickly detected. Importantly, by providing the opportunity to reduce CA levels by affecting different molecules, the siRNA approach allowed us to confirm if the effects in the invasiveness properties of dysplasia cells is in fact a consequence of the reduction in the number of centrioles, and not just due to the dysfunction of specific molecules. Indeed, while results obtained with 2D migration and invasion assay were mostly inconclusive and further optimization is needed, we found that reduction of CA levels, with both approaches, reduced the invasiveness capacity of dysplasia cells in 3D cultures. Our findings therefore support a role for CA in promoting the invasiveness capacity in dysplasia, and provided important clues into their mechanisms that will be explored in the future. We then tested if an increase in CA is sufficient to induce invasion in metaplasia cells. To do this we first depleted p53 in metaplasia cells by siRNA, already known to increase CA in these cells, and then assessed their behavior using 3D cell cultures. Interestingly, our preliminary tests did not reveal any phenotypic differences in metaplasia cells with increased CA when compared to the controls. These findings indicate that increasing CA levels in metaplasia may not be sufficient, by itself, to induce an invasive capacity in metaplasia cells. In the future, testing different approaches to induce CA in these cells, as well as assessing their impact in cell migration and invasion using other assays, will be important to confirm this.

By showing that CA contributes to the invasiveness potential in dysplasia, our results reveal the importance of CA in the acquisition of malignant properties in BE progression. These findings may contribute to new clinical tools, namely using CA as a biomarker of progression. Given widespread occurrence of CA in human tumors, our results may be extended to other cancers where CA is prevalent.

Keywords: Human cancer, Barrett's esophagus, Centrosome amplification, Invasion, Tumor progression

RESUMO ALARGADO

De forma a poder tratar o cancro é importante compreender as diferenças entre células normais e células tumorais. Uma destas diferenças está na desregulação dos centrossomas. Estas anomalias têm sido encontradas em diversos tipos de tumores, sugerindo uma possível função na formação e progressão tumorais. Porém, é ainda pouco claro se estas alterações são uma causa ou uma consequência do cancro.

O centrossoma é o principal centro organizador de microtúbulos nas células animais, desempenhando funções importantes na divisão, sinalização, polaridade e migração celulares. É um organelo composto por dois centríolos, centríolo mãe e centríolo filha, rodeados por uma matriz densa e organizada de proteínas, chamada material pericentriolar (PCM). O número de centríolos apresenta uma regulação muito precisa em células em proliferação, em estreita coordenação com o ciclo celular. No início do ciclo celular, na fase G1, a célula tem apenas um centrossoma, com dois centríolos. Na fase seguinte, fase S, tem início a duplicação do centrossoma, um processo regulado por diversas proteínas, incluindo a PLK4, SAS6 e STIL. Este processo baseia-se na formação de um novo centríolo na base de cada centríolo pré-existente. Durante a fase G2 da divisão celular, estes dois novos centríolos crescem e atingem o seu comprimento final na transição para a mitose. É na mitose que os dois centrossomas maturam e se separam, cada um com um centríolo mãe e um filha, migrando para polos opostos da célula e nucleando os microtúbulos que formam o fuso mitótico.

Falhas neste processo de duplicação, devido à desregulação de componentes importantes no processo, podem levar a defeitos centrossomais. Estas anomalias podem ser estruturais, relacionadas com o tamanho e composição dos centríolos e/ou do PCM, ou numéricas, caracterizadas por um ganho ou perda do número centríolos. A amplificação do número de centrossomas é a anomalia centrossomal mais frequentemente detetada no cancro mas o pouco conhecimento da sua origem e impacto na formação e progressão dos tumores tem limitado o seu uso na clínica. Para este tipo de estudos, é fundamental ter um modelo de cancro humano que permita o estudo dos diferentes estadios da doença e assim desvendar a presença e incidência destas anomalias em cada fase da doença, quais são os mecanismos subjacentes a essa amplificação e qual o seu papel na transformação maligna. Um excelente modelo de cancro humano é a tumorigénese do esófago de Barrett. Este modelo permite o estudo dos vários estadios de progressão tumoral devido ao fácil acesso a amostras desde a condição pré-maligna à metástase, mas também ao acesso a um painel validado de linhas celulares representativas destes estadios.

O esófago de Barrett (EB) é uma condição pré-maligna em que o epitélio escamoso estratificado normal do esófago é substituído por um epitélio colunar metaplásico semelhante ao estômago/intestino, sendo a sua principal causa o refluxo gastroesofágico. Esta alteração metaplásica é clinicamente relevante pois pode evoluir para adenocarcinoma do esófago, apesar de com uma baixa probabilidade. A evolução para neoplasia é um processo com etapas conhecidas que vão da metaplasia (EB), à displasia, adenocarcinoma e metástase. Nem todos os doentes com EB evoluem para adenocarcinoma. Porém, dado o elevado risco de progressão, estes doentes são incluídos em programas de vigilância onde biópsias endoscópicas periódicas permitem a avaliação da evolução da doença. O recente estudo do nosso laboratório revelou que a amplificação dos centrossomas surge cedo na condição pré-maligna, que esta aumenta significativamente na displasia e que só foi detetada em pacientes que progrediram para neoplasia, sugerindo a sua possível função na promoção da progressão e transformação do EB. Assim, colocámos a hipótese de que a amplificação dos centrossomas possa promover a progressão tumoral através da aquisição de propriedades malignas. Se esta hipótese estiver correta, então um

aumento da amplificação do número de centrossomas na metaplasia e/ou uma diminuição na displasia seriam suficientes para promover ou reduzir respetivamente as propriedades malignas.

Um dos mecanismos pelos quais a amplificação dos centrossomas pode levar à neoplasia é o ganho de propriedades invasivas. Sabe-se que as células de displasia possuem esse potencial invasivo, enquanto as células de metaplasia não têm este potencial. Assim, colocámos a hipótese de que a amplificação dos centrossomas poderia contribuir para a capacidade de invasão na progressão do EB. Para testar esta hipótese delineámos duas estratégias complementares: i) reduzir os níveis de amplificação dos centrossomas em células de displasia e avaliar alterações na sua capacidade migratória e invasiva, e ii) aumentar os níveis de amplificação dos centrossomas em células de metaplasia e avaliar a transformação, tal como aquisição de uma capacidade invasiva.

Para testar estas hipóteses, primeiro testámos dois métodos diferentes para reduzir os níveis de amplificação do número de centrossomas em células de displasia: depleção de moléculas importantes no ciclo de duplicação do centrossoma - PLK4, SAS6 e STIL - por siRNA e inibição da atividade de PLK4 usando um inibidor químico específico, centrinone-B. Em seguida, avaliámos as alterações na migração e potencial invasivo usando ensaios de migração e invasão 2D e culturas de células 3D. Ambas as estratégias foram eficazes na redução dos níveis de amplificação de centrossomas em células com displasia mas o tratamento com o inibidor, atuando diretamente na atividade da proteína, teve um efeito que foi detetado mais rapidamente. É importante salientar que, ao reduzir os níveis de amplificação dos centrossomas através da manipulação de diferentes moléculas, a abordagem de siRNA permite-nos confirmar se os efeitos nas propriedades de invasão das células de displasia são de fato uma consequência da redução no número de centríolos, e não apenas devido à disfunção de moléculas específicas. De fato, embora os resultados obtidos com a migração 2D e o ensaio de invasão tenham sido em sua maioria inconclusivos e uma otimização adicional seja necessária, descobrimos que a redução dos níveis de amplificação dos centrossomas, com ambas as abordagens, reduziu a capacidade de invasão das células de displasia em culturas 3D. Estes resultados apoiam, portanto, um papel da amplificação dos centrossomas na promoção da capacidade de invasão em displasia e forneceram pistas importantes sobre os seus mecanismos que serão explorados no futuro. Em seguida, testámos se um aumento da amplificação dos centrossomas é suficiente para induzir a invasão em células de metaplasia. Para isso, primeiro depletámos o p53 em células de metaplasia por siRNA, já conhecido por levar a um aumento dos níveis de amplificação de centrossomas nestas células, e em seguida avaliámos o seu comportamento usando culturas de células 3D. Curiosamente, os nossos testes preliminares não revelaram nenhuma diferença fenotípica em células de metaplasia com níveis elevados de amplificação dos centrossomas. Estes resultados indicam que o aumento dos níveis de amplificação na metaplasia poderá não ser suficiente, por si só, para induzir uma capacidade invasiva nas células de metaplasia. No futuro, testar diferentes abordagens para induzir os níveis de amplificação dos centrossomas nestas células, bem como avaliar seu impacto na migração e invasão celular usando outros ensaios, será importante para confirmar estes resultados.

Ao mostrar que a amplificação dos centrossomas contribui para o potencial invasivo em displasia, os nossos resultados revelam a importância desta amplificação na aquisição de propriedades malignas na progressão do EB. Estes resultados podem contribuir para o desenvolvimento de novas ferramentas clínicas, nomeadamente o uso da amplificação dos centrossomas como um biomarcador de progressão. Dada a ampla ocorrência de amplificação dos centrossomas em tumores humanos, estes resultados podem ser estendidos a outros cancros onde esta anomalia é prevalente.

Palavras-chave: Cancro humano, Esófago de Barrett, Amplificação do centrossoma, Invasão, Progressão do tumor

TABLE OF CONTENTS

ACKNOWLEDGMENTS ..... **II**
ABSTRACT ..... **III**
RESUMO ALARGADO ..... **IV**
TABLE OF CONTENTS ..... **VII**
LIST OF FIGURES ..... **IX**
LIST OF TABLES ..... **X**
LIST OF ABBREVIATIONS ..... **XI**

1. INTRODUCTION **1**

1.1 The centrosome 1
1.1.1 The centrosome structure 1
1.1.2 The centrosome duplication cycle 1
1.1.3 The centrosome function 2
1.2 Centrosome abnormalities and cancer 3
1.2.1 Causes of centrosome amplification 3
1.2.2 Consequences of centrosome amplification 3
1.3 A human cancer model to study centrosome amplification 5
1.3.1 Barrett's esophagus tumorigenesis 5
1.3.2 Barrett's esophagus and centrosome amplification 5
1.4 Objectives 6

2. MATERIAL AND METHODS **7**

2.1 Cell culture 7
Cell lines 7
siRNA transfection 7
Centrinone treatment 7
3D cell culture 7
Wound healing assays 8
Transwell assays 8
2.2 2D Immuofluorescence microscopy 8
Immunostaining 8
Antibodies 8
Image analysis 8
Centriole scoring 8
2.3 3D Immuofluorescence microscopy 9
Immunostaining 9
Antibodies 9
Image analysis 9
Invasion analysis 9
2.4 Western Blot 9
Cell lysis, SDS-PAGE and transfer 9
Protein detection 10
Quantification 10

2.5 Flow cytometry ….…… 10
2.6 qRT-PCR …… 10

3. RESULTS..... 10

3.1 The impact of reducing centrosome amplification in the migratory and invasiveness capacity of dysplasia cells ……..... 11
3.1.1 Reducing centriole numbers by siRNA transfection in dysplasia cells …… 11
3.1.1.1 Depletion of core centriolar proteins reduces centriole amplification in dysplasia cells ……. 11
3.1.1.2 2D migration and invasion assays did not reveal conclusive differences in the migration and invasive properties of dysplasia cells with reduced levels of CA ……..… 12
3.1.1.3 3D cell cultures showed a possible role of CA in the invasiveness capacity of dysplasia cells ……..... 17
3.1.2 Reducing centrosome amplification in dysplasia through chemical inhibition …… 18
3.1.2.1 Centrinone-B reduces centriole amplification in dysplasia cells ……..…… 18
3.1.2.2 2D migration and invasion assays did not show an impact in migration and invasive properties of dysplasia cells with reduced levels of CA through a specific inhibitor ……..… 19
3.1.2.3 3D cell cultures showed a reduction in the invasiveness potential in dysplasia cells treated with the chemical inhibitor ……..... 21
3.2 The impact of increasing centrosome amplification in the migratory and invasiveness capacity of metaplasia cells ……..…… 24
3.2.1 Increasing centriole numbers in metaplasia by depleting p53 through siRNA transfection …… 24
3.2.1.1 Depletion of p53 increases the centrosome amplification levels, in metaplasia cells …… 24
3.2.1.2 3D cell cultures suggest that centrosome amplification is not sufficient to induce invasiveness in metaplasia cells ……..…… 24

4. DISCUSSION 26

5. CONCLUSION AND FUTURE PERSPECTIVES 29

6. REFERENCES 29

7. SUPPLEMENTARY FIGURES 34

LIST OF FIGURES

Figure 1.1 - Centrosome structure and duplication cycle 2

Figure 1.2 - Mechanisms by which centrosome abnormalities can promote invasive phenotypes 4

Figure 1.3 - Barrett's Esophagus progression and centrosome amplification 6

Figure 3.1 – Depletion of core centriole biogenesis proteins reduces CA in dysplasia cells 12

Figure 3.2 – Migration and invasion assays with CP-B cells with reduced CA by depleting core centriole protein by siRNA..... 13

Figure 3.3 – Migration and invasion assays with CP-D cells with reduced CA by depleting core centriole protein by siRNA 14

Figure 3.4 – Optimized migration and invasion assays with CP-D cells with reduced CA by depletion of core centriole biogenesis proteins by siRNA 16

Figure 3.5 – Dysplasia cells with reduced CA through depletion of core centriole biogenesis proteins by siRNA showed a reduced invasiveness capacity in 3D cultures. 17

Figure 3.6 – Dysplasia cells exhibited increased CA levels after 3 days of continued treatment with centrinone 18

Figure 3.7 – Adding centrinone every 2 days leads to a reduction of CA levels in dysplasia. 19

Figure 3.8 – Migration and invasion assays in dysplasia cells with reduced CA through PLK4 inhibition by treated centrinone 20

Figure 3.9 – Dysplasia cells used for 3D cell cultures showed a reduction of CA through PLK4 inhibition by centrinone 21

Figure 3.10 – Dysplasia cells with reduced CA through PLK4 inhibition had a reduction in the invasive structures, in 3D cell cultures 23

Figure 3.11 – Metaplasia cells with increased CA, did not show differences in the invasiveness capacity, in 3D cultures..... 25

Figure S7.1 (Related to Figure 3.2) – Migration and invasion assays with CP-B cells with reduced CA by depleting core centriole protein by siRNA 34

Figure S7.2 (Related to Figure 3.3) – Migration and invasion assays with CP-D cells with reduced CA by depleting core centriole protein by siRNA 34

Figure S7.3 (Related to Figure 3.4) – Optimized migration and invasion assays with CP-D cells with reduced CA by depletion of core centriole biogenesis proteins by siRNA 35

Figure S7.4 – qRT–PCR showing the expression of SAS6 and STIL throughout BE progression …… 35

Figure S7.5 (Related to Figure 3.5) - Dysplasia cells with reduced CA through depletion of core centriole biogenesis proteins by siRNA showed a reduced invasiveness capacity in 3D cultures ……..... 36

Figure S7.6 (Related to Figure 3.9) – Migration and invasion assays in dysplasia cells with reduced CA through PLK4 inhibition by centrinone ……..……..……. 36

Figure S7.7 (Related to Figure 3.10) – Dysplasia cells used for 3D cell cultures showed a reduction of CA through PLK4 inhibition by centrinone ……..…….....… 37

Figure S7.8 – Bright-field microscopy showed a reduction in the invasiveness capacity of dysplasia cells, treated with centrinone, in 3D cultures ……..…..… 38

Figure S7.9 (Related to Figures 3.10 and 3.11) – Inhibition of PLK4, by centrinone, increased ploidy in dysplasia cells ……...…… 38

Figure S7.10 (Related to Figure 3.12) – Metaplasia cells with increased CA, did not show differences in the invasiveness capacity, in 3D cultures ……..…….. 39

LIST OF TABLES

Table 2.1 - Primer sequences used in the qRT-PCR ……...…….. 10

LIST OF ABREVIATIONS

2D	**T**wo-**d**imensional
3D	**T**hree-**d**imensional
BE	**B**arrett's **e**sophagus
BPE	**B**ovine **p**ituitary **e**xtract
CA	**C**entrosome **a**mplification
CIN	**C**hromosomal **In**stability
CP110	**C**entrosomal **p**rotein 110
CPAP	**C**entrosomal **p**rotein 4.1-**a**ssociated **p**rotein
DMSO	**Dim**ethyl **s**ulf**o**xide
EGF	**E**pidermal **g**rowth **f**actor
EMT	**E**pithelial-to-**m**esenchymal **t**ransition
FBS	**F**etal **b**ovine **s**erum
GAPDH	**G**lycer**a**ldehyde-3-**P**hosphate **De**h**h**ydrogenase
GL2	Luciferase
IF	**I**mmuno**f**luorescence
mRNA	**m**essenger **RNA**
MTOC	**M**icro**t**ubule **o**rganizing **c**entre
MTs	**M**icro**t**ubules
PBS	**P**hosphate **b**uffered **s**aline
PCM	**P**eri**c**entriolar **m**aterial
PLK1	**P**olo-**l**ike **k**inase 1
PLK4	**P**olo-**l**ike **k**inase 4
qRT-PCR	reverse transcriptase **q**uantitative **R**eal-**T**ime **P**olimerase **C**hain **R**eaction
RNA	**R**ibo**n**ucleic **a**cid
RT	**R**oom **t**emperature
SAS6	**S**pindle **as**sembly abnormal protein 6 homolog
SDS-PAGE	**S**odium **d**odecyl **s**ulfate **p**oly**a**crylamide **g**el **e**lectrophoresis
siRNA	**s**mall-**i**nterfering **RNA**
STIL	**S**CL/**T**AL-1-**i**nterrupting **l**ocus protein
TBS	**T**ris **B**uffered **S**aline
WB	**W**estern **b**lot
WT	**W**ild-**t**ype

1. INTRODUCTION

To treat cancer, it is important to understand the differences between normal cells and tumor cells. Centrosome abnormalities are one of these differences and have been found in a variety of tumors, suggesting a possible role in tumor initiation. However, it remains unclear whether these aberrations are a cause or consequence of cancer[1].

1.1 The centrosome

The architecture and motility of eukaryotic cells are sustained by the dynamic and interconnected networks of the cytoskeleton, including actin and microtubules (MTs)[2,3]. In a cell, MTs are associated with microtubule organizing centers (MTOCs), being the centrosome the primary MTOC in animal cells[4]. The centrosome was first described by Theodor Boveri (1887) as the special cell division organ[5]. Boveri also proposed that an excessive number of centrosomes during mitosis promoted the formation of multipolar spindles, leading to aneuploidy that would trigger tumorigenesis[1]. This theory was outlined more than 100 years ago and, for many years, researchers focused on the discovery of mutations in oncogenes and tumor suppressor genes as the drivers of tumorigenesis. The interest in centrosome defects returned with the observation that loss of the tumor suppressor p53 was associated with centrosome amplification[6]. As a result, several studies have been done over the past two decades in order to better understand the association between centrosome abnormalities and malignancy.

1.1.1 The centrosome structure

The centrosome is composed of two centrioles surrounded by a dense and highly structured matrix of proteins termed the pericentriolar material (PCM) (Figure 1.1 A). Centrioles are highly conserved MT-based cylinders of approximately 500 nm in length and 250 nm in diameter, and with a 9-fold radial symmetry[7,8]. Each member of the pair of centrioles differs structurally and functionally. The fully mature centriole, known as the mother centriole, is the older one in the pair and is distinguished by the presence of two sets of nine appendages (subdistal and distal appendages). The immature and younger centriole, the daughter centriole, is about 80% the length of the mother centriole and does not present appendages[9]. Both centrioles nucleate MTs but only the mother centriole can anchor MTs at the subdistal appendages[7]. The PCM is a dynamic and highly organized structure composed of hundreds of proteins, including proteins implicated in MT nucleation such as pericentrin, γ-tubulin as well as other tubulins, motor proteins and regulatory molecules[10].

1.1.2 The centrosome duplication cycle

To ensure cellular homeostasis the number of centrosomes throughout the life cycle of a cell is tightly regulated. During cell division the centrosomes must duplicate, in coordination with the cell cycle, to assure the formation of a bipolar spindle and that each daughter cell inherits a single correctly assembled centrosome at the end of cell division. The centrosome duplication cycle is therefore regulated by two golden rules: the new centriole is only formed next to a pre-existing one and each centriole duplicates only once per cell cycle. This regulation will assure the correct number of centrioles per cell[11] (Figure 1.1 B). Briefly, newly born cells at early interphase in G1, have one centrosome, with a pair of centrioles, a mother and a daughter centriole, loosely connected by linker fibers[8]. At late G1 and early S phase, the formation of new centrioles start with CEP152 recruiting PLK4, the master regulator of centriole biogenesis, to each pre-existing centriole. PLK4 then recruits and phosphorylates

STIL, which then facilitates SAS6 binding. STIL and SAS6 are essential for cartwheel formation in the procentrioles (the new forming centrioles), and only one procentriole is formed next to the parental centriole[8,12–14]. During S and G2 phases, each new procentriole elongates, in a process regulated by several proteins such as CP110 and CPAP[15,16]. By late G2 the new fully elongated and formed daughter centrioles are orthogonally positioned and engaged (tightly connected) to their mothers[8,9,17]. This engagement is essential to prevent re-duplication. At this point, the cell has two centrosomes, and the daughter centriole of the original pair will now become a mother centriole. When cells transition from the G2 phase to mitosis, this new mother centriole loses the previous linker fiber connection with the older centriole which results in the separation of the two centrosomes. During this transition the centrosomes also start accumulating PCM, which allows them to nucleate more MTs and thus form the mitotic spindle. This process is called centrosome maturation and is regulated by two kinases, PLK1 and Aurora A[9,17]. As cells exit mitosis and enter early G1, the two pairs of mother and daughter centrioles disengage, and start to be connected only by the linker fibers again. This process, called centriole disengagement, is dependent on PLK1 and separase[18] and is crucial to allow duplication in the following cell cycle. It is also at this time that the new mother acquires the full set of distal and subdistal appendages. Afterwards, a new cycle begins[8,9].

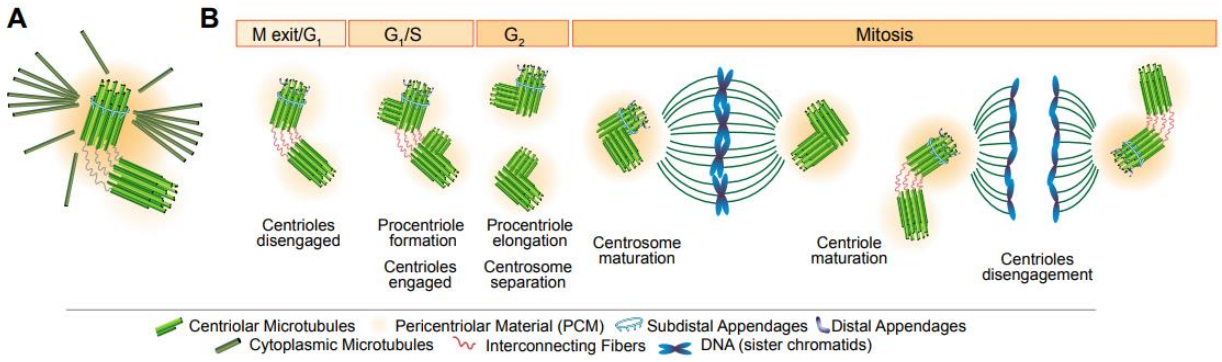

Figure 1.1 Centrosome structure and duplication cycle. (A) The centrosome is composed of two MT-based centrioles surrounded by a dense and highly structured mass of proteins termed the pericentriolar material (PCM). **(B)** Centrosome duplication cycle is tightly regulated within the cell cycle. Each centriole duplicates only once per cell cycle, and only one centriole is formed next to a pre-existing one.

1.1.3 The centrosome function

As the primary MTOC in animal cells, the centrosome coordinates a variety of processes such as spindle assembly, intracellular signaling and trafficking, the establishment of cell polarity, and cell motility[9]. The centrosome is important in cell division to nucleate microtubules and form the bipolar mitotic spindle, which is responsible for correct chromosome segregation[17]. Centrosomes are also important in post-mitotic and differentiated cells where they can adopt specific positions and organize MT arrays that are important for determining the shape, polarity, and motility of cells[19]. This organelle also plays an important function during ciliogenesis. During this process, centrosomes migrate to the apical plasma membrane where the mother centriole docks, through the distal appendages, becoming a basal body that nucleates the formation of cilia[10]. Centrosomes may also function as hubs for the integration of signaling pathways, such as cell cycle progression and DNA damage response[20,21]. In order to ensure the correct functions of centrosomes, their number, structure and composition are highly regulated. In fact, abnormalities in centrosome numbers or structure have been associated with serious pathologies, such as ciliopathies, microcephaly and cancer[19,22].

1.2 Centrosome abnormalities in human cancer

In cancer, centrosomal abnormalities have been identified in a variety of solid tumors, such as breast, prostate, colon, ovarian and pancreatic cancer, and also in hematological malignancies[1,23]. Centrosomal abnormalities are generally classified as structural or numerical aberrations[1]. Structural aberrations are characterized by defects in centriole size or composition and also PCM structure. These alterations most likely arise due to deregulated expression of genes coding for centrosomal components or altered post-translational modifications[24]. For example, depletion of CP110 has been shown to lead to overly long centrioles[16].Numerical abnormalities are characterized by either loss or gain of centrosomes. The gain of centrosomes, or centrosome number amplification (CA), is the most frequent defect detected in human cancer[23]. This centrosomal abnormality is the main focus of this thesis and will therefore be discussed in more detail.

1.2.1 Causes of centrosome amplification

One major source of CA is the deregulation of the centrosome duplication cycle, namely by the overexpression of centriolar or PCM components[1]. A well-described example is the deregulation of the main molecules involved in centriole biogenesis, PLK4, STIL and SAS6: while their overexpression can lead to supernumerary centrioles, their depletion can impair centriole duplication[1,24]. CA can also originate from cell cycle defects. For example, cytokinesis failure or mitotic slippage can lead to the formation of tetraploid cells and simultaneously CA[1]. It is not clear which of these mechanisms have a more prevalent role in generating CA in human cancers, and it may differ according to the considered tumor.

1.2.2 Consequences of centrosome amplification

CA is a hallmark of human cancer[1]. Whether this abnormality has a role in tumor initiation has been a subject of interest for many decades, with several studies addressing this hypothesis. Recently, it was shown that CA is sufficient to promote spontaneous tumorigenesis in mice[25]. However, it is still unknown whether they are a cause or consequence of human tumorigenesis[1]. To understand how CA could be influencing tumorigenesis and tumor progression, it is necessary to analyze its consequences in cellular homeostasis. It is during mitosis that its best-studied consequence occurs. Untransformed normal cells with supernumerary centrosomes will form multipolar spindles that lead to severe levels of aneuploidy that likely result in cell death. However, cancer cells have developed coping mechanisms to avoid cell death upon cell division with CA. One of such mechanisms consists in clustering their supernumerary centrosomes into two poles and form a pseudo-bipolar mitotic spindle that will allow the generation of viable daughter cells[1,22,26]. However, while clustering their extra centrosomes, cells form transient multipolar spindles that can lead to merotelic attachments (erroneous connections between MTs and kinetochores) that will result in lagging chromosomes[1,22,26]. This will generate chromosomal instability (CIN) that may contribute to the loss of certain tumor suppressor genes or gains of oncogenes, and therefore providing cells with CA a proliferative advantage over cells with normal centriole numbers[27]. It is also becoming clear that the role of extra centrosomes is not limited to mitosis. In interphase cells, CA may contribute to defective ciliary signaling, possibly through formation of ectopic primary cilia. In fact, super-ciliated cells due to CA have been reported in multiple tissues and cell types[19,28]. Supernumerary centrosomes could also affect signaling pathways by promoting the accumulation of signaling molecules at centrosome clusters making it easier to be activated[1]. Importantly, increased MT nucleation resulting from the presence of an increased number of centrosomes has been shown to alter migration and invasive behavior of cells[29]. These observations reveal that CA may play a role in tumor initiation and progression. Despite all of the progress made,

little is known about the impact of CA in human cancer. As the impact of CA in the migratory and invasiveness capacity is the main focus of this thesis, this will be discussed in more detail.

Invasion, a hallmark of malignancy, is the first step of metastasis and refers to the ability of cancer cells to escape the site of the primary tumor and enter into surrounding normal tissue[30]. During cancer progression, a variety of tumor cells show changes in their plasticity by morphological and phenotypical conversions, including the epithelial to mesenchymal transition (EMT)[30,31]. EMT is a normal and important process during development[32]. However, cancer cells subvert this program to their own benefit, and during the last decade it has been increasingly recognized as a crucial event in tumor initiation and invasion, and it is a key initiating step in metastasis[30]. EMT is characterized by loss of epithelial characteristics, such as expression of epithelial E-cadherin, and the gain of mesenchymal markers such as vimentin, fibronectin and neuronal N-cadherin[30,33,34]. This change in expression leads to enhanced motility of transformed cells, losing their epithelial organization and gaining the ability to detach from epithelial cell clusters and move as single cells, just like mesenchymal cells[33,34]. Some studies showed that CA may contribute to invasive properties due to changes in the EMT, showing that the knockdown of PLK4 suppressed migration and invasion by reducing the expression of mesenchymal markers, leading to an inhibition of EMT[37–39]. Recent work has uncovered other mechanisms by which CA may contribute to metastasis by facilitating invasion (Figure 1.2). Using 3D cell cultures, a study with non-transformed human mammary epithelial cells (MCF10A) showed that CA, triggered by overexpression of PLK4, promoted an increase in MT nucleation capacity. This increase leads to Rac1 signaling and actin polymerization, weakening E-cadherin junctions and promoting the formation of invasive protrusions in cells with extra centrosomes[29,30]. In addition to promoting the formation of invasive protrusions through a cell-autonomous effect, a non-cell autonomous effect is also observed, when conditioned media with pro-invasive factors secreted from cells with extra centrosomes promoted the formation of protrusions in 3D organoid cultures of cells with normal centrosome numbers[30,40]. With this, tumor cells can benefit from the centrosome aberrations present in only a subset of cells in the tumor population. Other centrosome aberrations, such as structural abnormalities, may also contribute to this invasive capacity. These abnormalities, induced by overexpression of Nlp, lead to increased MT nucleation and stability and this increases interphase stiffness and disrupts E-cadherin junctions promoting the extrusion from the epithelium[30,41].

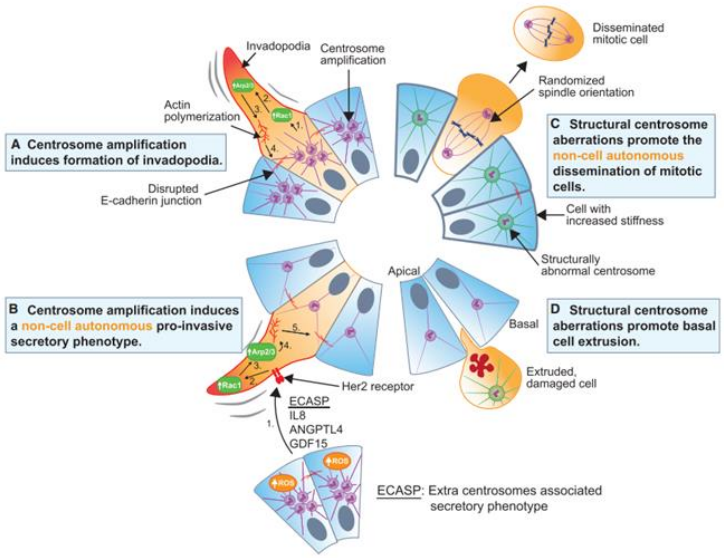

Figure 1.2. Mechanisms by which centrosome abnormalities can promote invasive phenotypes. Centrosome amplification can induce the formation of invadopodia and a non-cell autonomous pro-invasive secretory phenotype. Also, structural centrosome abnormalities can promote non-cell autonomous dissemination of mitotic cells and basal cell extrusion. (Adapted from LoMastro and Holland, 2019.)

1.3 A human cancer model to study centrosome amplification

Given the association of CA with multiple cancer types, it is important to study its origin and impact in human tumor progression. For that, it is essential to have a human cancer model that allows the study of the different stages of disease to uncover when CA emerges, what are the mechanisms underlying this amplification, and what is the role of CA in malignant transformation and progression. Barrett's esophagus tumorigenesis is an excellent model of human cancer not only due to the fact that we have access to samples of all stages of disease (from pre-malignant condition to metastasis) but also access to a validated panel of cell lines representing all these stages and that can be manipulated to test hypotheses.

1.3.1 Barrett's esophagus tumorigenesis

Barrett's esophagus (BE) is a premalignant condition in which the normal stratified squamous epithelium of the esophagus is replaced by a stomach/intestine-like metaplastic columnar epithelium[42]. The main risk factor for the development and progression of BE is chronic gastroesophageal reflux[43], being this reflux the retrograde movement of stomach contents into the esophagus. This repetitive exposure to acids and bile salts causes prolonged injury to the esophageal epithelium. Although the mechanisms underlying these changes remain unknown, some models and hypotheses for its origin have been proposed. These include the direct conversion of esophageal cells to metaplastic cells, undifferentiated gastric cells from the cardia, relocation of submucosal esophageal gland ducts, circulating bone marrow cells that colonize the damaged esophagus, and the transitional epithelium that has both squamous and columnar features[44–47].

This metaplastic change is clinically relevant because patients with BE have an increased risk of developing esophageal adenocarcinoma[48]. Its neoplastic progression is a process with well-characterized and defined steps that go from metaplasia (premalignant condition - BE) to dysplasia (low- or high-grade intraepithelial neoplasia), adenocarcinoma (invasive neoplasia) and metastasis[49,50] (Figure 1.3 A). Importantly, not all BE patients progress to adenocarcinoma, with progression probabilities of 0.1%-0.3% per year[51,52]. As a result, and given the increased risk of BE patients to progress to adenocarcinoma, BE patients are included in a surveillance program, where periodic endoscopic biopsies allow the assessment of the evolution of disease[48]. The diagnosis is confirmed by the presence of morphological changes indicative of dysplasia in patient's biopsies. Besides such morphological changes, there are currently no biomarkers available to determine which patients will progress and which will not. So, there is a clinical need for such biomarkers.

1.3.2 Barrett's esophagus and centrosome amplification

Our lab has recently shown when CA arises in BE progression, as well as its incidence throughout the progression, using patient samples and representative cell lines[49]. This work showed that CA arises as early as the pre-malignant condition and, importantly, that CA was only detected in samples of BE that progressed to neoplasia and never in samples of non-progressed patients (Figure 1.3 B and C). Moreover, CA was detected in all subsequent steps of progression, and its incidence significantly increased from metaplasia to dysplasia. This increase was dependent on loss of wild-type function of the tumor suppressor p53 (Figure 1.3 C), the most commonly mutated gene in human cancer[53]. Together,

these findings strongly suggest that CA could play an important role in tumor initiation and progression in BE.

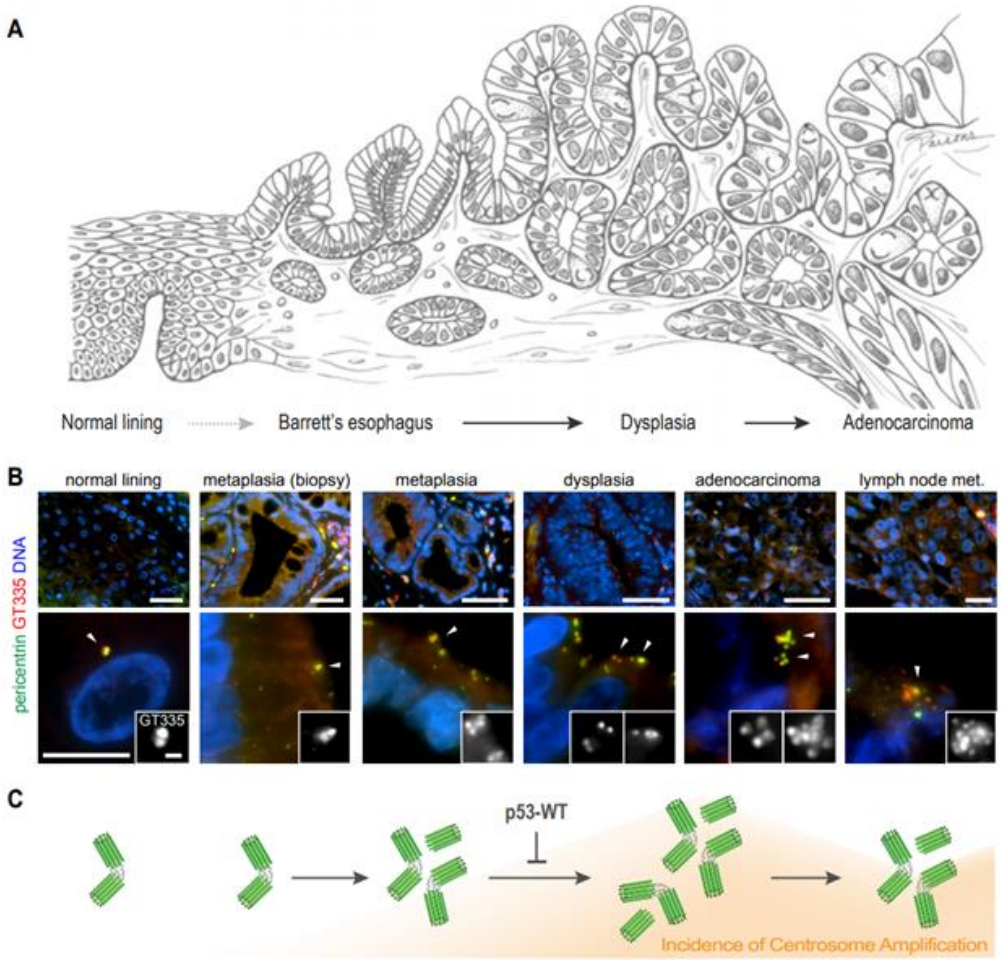

Figure 1.3. Barrett's Esophagus progression and centrosome amplification. (A) Schematic representation of Barrett's esophagus neoplastic evolution, a process with defined steps that go from metaplasia to dysplasia, adenocarcinoma and metastasis. **(B-C)** The analysis of centrosomes in clinical samples (representative immunofluorescence images are shown in B) and representative cell lines revealed that CA arises in metaplasia and its incidence changes through disease progression. The significant increase in the incidence of CA from metaplasia to dysplasia transition is dependent on loss of wild-type (WT) p53 function (schematic representation of these findings is shown in C). (Adapted from Lopes et al, 2018.)

1.4 Objectives

The observations that CA arises in BE metaplasia, that it was only detected in patients that progressed to neoplasia[49], and its incidence significantly increased in the transition from metaplasia to dysplasia (intra-epithelial neoplasia), strongly suggested that CA plays an important role in tumor formation. We therefore posed the hypothesis that CA could promote BE progression by contributing to the acquisition of malignant properties. Particularly, given the increased risk of dysplasia to progress to invasive neoplasia[50], and that dysplasia cells have migratory and invasiveness potential[54], we aimed to understand if CA contributes to BE progression by promoting such migratory or invasive potential. To test this hypothesis, two complementary approaches were envisioned: i) to increase the levels of CA in metaplasia cells and assess its sufficiency to promote the acquisition of invasiveness potential; and ii) to reduce CA levels in dysplasia cells and assess its sufficiency to hamper their invasiveness potential. To increase or reduce centrosome numbers we interfered with the levels or activity of known key regulators of centrosome biogenesis. After testing and optimizing each of these approaches, we then performed different assays to assess changes in migration and invasion.

2. MATERIAL AND METHODS

2.1 Cell Culture

Cell lines. Human telomerase-immortalized (hTERT) BAR-T cell lines derived from biopsies of patients with nondysplastic BE (from R. Souza, Baylor Univ. Medical Center, Dallas) were cocultured with a fibroblast feeder layer (Swiss 3T3 cells) treated with 10 µg/ml mitomycin C (Sigma) for 2h and maintained in KBM2 medium (Lonza) supplemented with 5% fetal bovine serum (FBS), 0.1 nM cholera toxin (Sigma), 70 µg/ml bovine pituitary extract (BPE; Thermo Fisher), 400 ng/ml hydrocortisone (Sigma), 20 ng/ml epidermal growth factor (EGF; Sigma), 20 µg/ml adenine (Sigma), 5 µg/ml insulin (Sigma), 5 µg/ml transferrin (Gibco), and 100 U/ml penicilin-streptomycin-amphotericin (PSA; Thermo Fisher). When seeding these cells for individual experiments, wells were precoated with collagen IV (1µg/cm^2; Sigma). hTERT CP-B, CP-C and CP-D cell lines derived from biopsies of patients with high-grade dysplasia (from P. Rabinovitch, Univ. of Washington, Seattle) were maintained in MCDB 153 medium (Sigma) supplemented with 5% FBS, 4 mM L-Glutamine (Thermo Fisher), 0.1% Insulin-transferrin-sodium-selenite (Sigma), 100 U/ml PSA, 140 µg/ml BPE, 20 µg/ml adenine, 0.4 µg/ml hydrocortisone, 1 nM cholera toxin and 20 ng/ml EGF. Cells were grown at 37ºC and with a 5% CO_2 atmosphere.

siRNA transfection. Endogenous *PLK4, SAS6* and *STIL* were individually depleted using siRNA oligonucleotides (Sigma) (PLK4: 5'-GGTGAAAATACATTGCCAATT-3'; SAS6: 5'-GCACGTTAATCAGCTACAA-3'; STIL (5'-GTTTAAGGGAAAAGTTATT-3'). Endogenous *TP53* was depleted using 3 siRNA oligonucleotides (*TP53*[1]: 5'-GGGAGTTGTCAAGTCTCTG-3', Sigma; *TP53*[2]: sc-29435; Santa Cruz); *TP53*[3]: 5'-GACTCCAGTGGTAATCTAC-3', Sigma). As controls, cells were either mock-treated (cells treated with all reagents for the transfection, except the siRNA oligonucleotides), or transfected with luciferase (*GL2*) siRNA (5′-CGTACGCGGAATACTTCGA-3′, Sigma). Cells were seeded and only after 24 hours (h) transfected with 50 nM siRNA, using Lipofectamine RNAiMAX (Thermo Fisher) according to manufacturer instructions. After 72h or 96h of transfection, cells were fixed for analysis of centriole numbers by immunofluorescence (see below for details). After 96h, cells were also collected for protein/RNA extraction or cell cycle profile and DNA content analysis by flow-cytometry. In the case of 3D culture assays, cells were re-transfected with siRNA oligonucleotides 3 days after the first transfection.

Centrinone treatment. Cells were seeded and 24h later were treated with 500nM of centrinone-B (in DMSO; Tocris Bioscience). Cells treated with DMSO (same volume as centrinone used) were used as negative control. Fresh media with inhibitor or DMSO was added to the cells every 2 days.

3D cell culture. The 3D cell culture was performed as previously described[29]. Briefly, a collagen-I (Corning) and matrigel (Corning) matrix mix was prepared as described and 42µl of this mix were added to each well of an 8-well chamber and incubated at 37ºC for 1h to polymerize. Cells (pretreated with centrinone or transfected with siRNA oligonucleotides) were resuspended with assay medium (growth medium as described above, but with 2% FBS) and 2% matrigel was added to the cell suspension just before plating. After 24h, cells were refed with assay medium containing 2% matrigel. Cells were incubated at 37ºC for 4 or 7 days and fixed for immunofluorescence microscopy. In the 7 days assay, cells were refed with assay medium containing 2% matrigel after 4 days. For the cells treated with centrinone, cells were refed with assay medium containing 2% matrigel and centrinone every 2 days.

Wound healing assays. Wound healing assays were performed using 2-well culture-inserts (Ibidi). Cells (pretreated with centrinone or transfected with siRNA oligonucleotides) were resuspended and 70 µL of cell suspension (with $7x10^5$ cells/mL) was seeded into each well of the insert. The insert was removed, to form the gap, and cell migration into the cell free gap was observed for 24h in specific time-points on Nikon Eclipse TS100 inverted bright-field microscope using the 10x objective. Image analysis was carried out using ImageJ by measuring the total wound area in three fields per condition, at time 0 (0h) and after 6, 12 and 24 h. Measurements at each location were averaged to yield a mean wound area. The wound area was expressed as a percent of wound closure, and compared between the different conditions.

Transwell assays. Cells (pretreated with centrinone or transfected with siRNA oligonucleotides) were serum-starved for 4h or 24h. Cells were resuspended in the same medium and $4x10^4$ cells seeded on the top chamber of transwell inserts (Corning) in 24-well plates, with or without matrigel-coated membranes with 0.8 µm pores. Standardized matrigel-coated inserts (Corning), were used, but concentrations of 0.5 and 2.5 mg/mL of matrigel were also tested. The bottom compartment of the chambers was filled either with standard full growth media or full growth media with 10% FBS. After incubation at 37°C in 5% CO2 for 24 h, noninvaded cells were wiped up with a cotton swab and the invaded cells were fixed with ice-cold methanol and stained with Hoechst 33342 (Invitrogen). 30 fields were selected using a Ti-E inverted microscope (Nikon) with the 40x objective, and the migrated and invaded cells were counted manually.

2.2 2D Immunofluorescence microscopy

Immunostaining. Cells grown on coverslips in 24-well plates were fixed and permeabilized with ice cold methanol at -20ºC for 10 minutes (min). After three washes (5 min each) with 1X Dulbecco's Phosphate Buffered Saline (PBS; Biowest) cells were blocked with 10% FBS in PBS (blocking solution) for 1h at room temperature (RT). Primary antibodies were diluted in blocking solution and incubated in a humidified chamber overnight at 4ºC. After washing (3 x 5 min) with PBS, cells were incubated with secondary antibodies diluted in blocking solution for 1h at RT in the dark. Before a final round of washes, cells were incubated with 1 µg/ml Hoechst 33342 in PBS for 10 min. Finally, coverslips were mounted on glass slides in VECTASHIELD Mounting Medium (Vector) and stored at 4ºC.

Antibodies. Primary antibodies used were against pericentrin (1:5000; rabbit; Abcam; ab4448) and centrin (clone 20H5; 1:500; mouse; Millipore; 04-1624). The secondary antibodies Rhodamine red (1:500; rabbit; Jackson ImmunoResearch Laboratories, Inc.) and Alexa Fluor 488 (1:500; mouse; Thermo Fisher Scientific) were also used.

Image Analysis. For immunofluorescence microscopy, images were obtained at RT using a Ti-E inverted microscope (Nikon) with a Plan Apochromat VC 100x 1.40 NA oil objective, an ORCA ER2 charge-coupled device camera (Hamamatsu Photonics), and Nikon software DAPI. The images were acquired as a z series (0.2 µm z interval) and are presented as maximum-intensity projections. Images were prepared using Photoshop (Adobe) and ImageJ (National Institutes of Health).

Centriole scoring. Centrioles were identified and scored through the centriole marker centrin when this colocalized with the PCM marker pericentrin. One hundred interphase mononucleated cells were analyzed in all conditions. As we did not co-stain cells with a cell cycle marker only cells with more than four centrioles (given by centrin staining) were considered to have centriole amplification.

2.3 3D Immunofluorescence microscopy

Immunostaining. The protocol was performed as previously described[29]. Briefly, cells grown in 3D cultures were washed with PBS and fixed with 5% formalin in PBS for 20 min at 37ºC. After fixation, cells were washed (3 x 10 min) with glycine buffer at RT, and permeabilized with 0.5% Triton X-100 in PBS at RT for 10 min. Cells were washed with IF wash buffer for 1h at RT. Cells were then blocked with 10% goat serum (Sigma) in IF wash buffer (blocking solution) for 1h at RT, and then incubated with primary antibodies diluted in blocking solution in a humidified box at 4ºC overnight. After washing (3 x 20 min) with IF wash buffer at RT, cells were incubated with secondary antibodies (in blocking solution) for 1h at RT in the dark. Cells were then washed (3 x 20 min) with IF wash buffer. Before a final round of washes, cells were incubated with 1:2500 Hoechst 33342 (Invitrogen) in PBS for 10 min at RT. Finally, slides were mounted with ProLong™ Gold Antifade Mountant (Thermo Fisher) and left to dry for 5 days at RT in the dark, and then stored at 4ºC.

Antibodies. Primary antibody used was against α-tubulin (1:500; mouse; Sigma, T9026). The secondary antibody Alexa Fluor 488 (1:500; mouse; Thermo Fisher Scientific) was also used.

Image Analysis. To follow possible cell proliferation and morphological modifications, cells were imaged at specific time points with a Nikon Eclipse TS100 inverted bright-field microscope using the 10x objective. For immunofluorescence microscopy, images were obtained at RT using a Ti-E inverted microscope (Nikon) with the 10x objective, an ORCA ER2 charge-coupled device camera (Hamamatsu Photonics), and Nikon software DAPI. The images were acquired as a z series (10 µm z interval) and are presented as maximum-intensity projections. Images were prepared using Photoshop (Adobe) and ImageJ (National Institutes of Health).

Invasion analysis. The analysis of cell invasiveness capacity was done by observing the α-tubulin staining and thus identifying cytoplasmic protrusions. 40 organoids per condition were characterized and organized into 3 major classes with sub-classes that would reflect their complexity and invasiveness phenotype: (i) single cells (organoids with only one cell) and single cells with protrusions; (ii) sphere-like clusters (organoids formed by more than one cell organized in a perfect round cluster) and sphere-like clusters with protrusions; (iii) non-sphere-like clusters (organoids formed by more than one cell organized randomly without a perfect conformation), non-sphere-like clusters with protrusions, and non-sphere-like clusters with tubules (organoids where the protrusions were organized and formed tubular structures). The number of cells per organoid was also analyzed.

2.4 Western Blot

Cell lysis, SDS-PAGE and transfer. Resuspended cells were pelleted before being snap frozen in liquid nitrogen, and then stored at -80ºC for posterior extraction. Cell lysates were prepared by resuspending pellets in lysis buffer (50 mM Hepes, pH 7.4, 100 mM KCl, 1 mM EGTA, 1 mM MgCl2, 10% glycerol, 0.05% NP-40, 1× protease inhibitor cocktail, and 1× phosphatase) for 20 min on ice. Lysates were then centrifuged for 10 min at 14,000 rpm at 4ºC. Protein concentration of the supernatant was determined by Bradford assay (Bio-Rad). Laemmli buffer was added to 60 µg of protein samples, which were then boiled at 95ºC for 5 min and then loaded on a pre-cast 4-12% gradient polyacrylamide gels (Invitrogen). The proteins present on the gel were transferred to nitrocellulose membranes by a semi-dry transfer method for 1h at 20 V. Blocking was done for 1h at RT in TBS with 5% milk powder and the antibody incubations were done overnight at 4ºC for primary antibodies and 1h at RT for secondary antibodies, in TBST 0.1% (Tween-20 [Sigma] in TBS) supplemented with 1% milk powder. Washes with TBST were done after each antibody incubation.

Protein detection. Primary antibodies used for western blotting were against fibronectin (1:500; mouse; Santa Cruz), SAS6 (1:500; mouse; Santa Cruz), STIL (1:500; rabbit; Bethyl), vimentin (1:200; mouse; Santa Cruz) and GAPDH (1:1000; rabbit; Cell Signalling). The secondary antibodies used IRdye 680CW (1:10000; mouse or rabbit; Li-COR) and IRdye 800CW (1:10000; mouse or rabbit; Li-COR) and membranes were developed and quantified on the Odissey Scanner (Li-COR).

2.5 Flow Cytometry

Cells were harvested, pelleted, and washed in 1× PBS. Pellets were then fixed with 70% ice-cold ethanol added drop-wise while slowly vortexing. After incubating on ice for 30 min, pellets were washed with 1xPBS before resuspending the fixed cells in a PI solution (1×PBS with 100 µg/ml RNase A and 100 µg/ml propidium iodide [Sigma]). Cells were then incubated in a water bath at 37ºC in the dark for 30 min and then kept at 4ºC until analysis. Flow cytometry was performed using the Fortessa X-20 (BD). Analysis of the results was done on the FlowJo software.

2.6 qRT-PCR

RNA was prepared using Qiagen RNAeasy kit according to the manufacturer's instructions. 1 µg of RNA was used to produce cDNA using High-Capacity RNA-to-cDNA™ Kit (ThermoFisher Scientific), according to the manufacturer's instructions. For qRT–PCR, we used Power SYBR Green followed by analysis with ABI QuantiStudio 7 Flex Real Time PCR (Applied Biosystems). All primers used for qRT-PCR are described in Table 2.1.

Table 2.1 - Primer sequences used in the qRT-PCR.

Gene symbol	Primer Forward 5'-3'	Primer Reverse 5'-3'
SAS6	GAATGGGCGTCACATACAGC	TTGATATTGAACCTGTGCCTGC
STIL	AATGAAGTCACAAGTCTTCCAGG	CACAACTAGAGAAGAGCTGTTGG

3. RESULTS

The observations that CA arises early in metaplasia, increases significantly in dysplasia, and that it was only detected in metaplasia from patients that progressed to neoplasia, suggest that CA may have a role in tumor initiation. Particularly, given that the levels of CA are higher in dysplasia cells, perhaps CA could promote BE progression by promoting the acquisition of malignant properties. One of the mechanisms through which CA can lead to tumorigenesis is the gain of invasive properties[22,55]. Importantly, it is known that dysplasia cells have a higher migratory and invasive capacity than metaplasia cells[54]. We therefore hypothesized that CA could contribute to the invasiveness capacity in BE progression. To test this hypothesis, we designed two complementary strategies: i) reduce CA levels in dysplasia cells and assess if that is sufficient to reduce their migratory and invasiveness potential, and ii) increase the levels of CA in metaplasia cells and assess if that is sufficient for their transformation, including acquisition of migratory and invasiveness potential. There are several assays that allow the assessment of migration and invasion properties of cultured cells, including the classic and commonly used 2D wound healing assays (to assess migration) and transwell assays (to either assess migration or invasion), commonly known as Boyden chamber assays[35]. The invasive properties of cells can also be assessed in 3D cultures. A previous study using non-transformed human mammary epithelial cells (MCF10A) in matrigel-derived 3D cultures showed that while untreated cells form perfect glands of cells that mimic the real anatomy of the mammary gland, cells with CA (induced by PLK4 overexpression) started to form invasive protrusions, cytoplasmic extensions that invade the surrounding matrix[29]. Notably, and in agreement with previous studies assessing the migratory or invasive properties

of BE-derived cell lines using classic 2D assays[54], preliminary data from our lab using such 3D cell cultures, showed that whereas metaplasia cells grow as contained clusters of cells (similar to untreated MCF10A cells), dysplasia cells mostly displayed a morphology reminiscent of invasive protrusions. We therefore decided to use all of these assays (wound healing, transwell and 3D cell cultures) to assess differences in the migratory or invasive properties of BE-derived cell lines upon reduction or increase of CA.

3.1 The impact of reducing centrosome amplification in the migratory and invasiveness capacity of dysplasia cells

We first asked if reduction of CA levels led to a reduction of the invasiveness capacity of dysplasia cells. To do this, we used three cell lines (CP-B, CP-C and CP-D) established from high-grade dysplasia samples (from three different patients). It is important to note that all three dysplasia cell lines have lost WT p53 function[56] and exhibit similar levels of CA[49]. To reduce CA, we hampered the ability of cells to normally duplicate their centrosomes. By inhibiting the production of new centrioles, the existing centrioles will be diluted in the cell population through successive cell divisions, which will eventually lead to an overall reduction of the incidence of CA. To achieve this, we blocked either the production (through siRNA) or function (through chemical inhibition) of key molecules for centriole duplication. Once the conditions of CA reduction were optimized, we then performed wound healing, transwell assays and 3D cell cultures to assess migration and invasion properties.

3.1.1 Reducing centriole numbers by siRNA transfection in dysplasia cells

In the first approach, we transfected dysplasia cells with specific siRNA oligonucleotides to reduce the expression of important molecules for centrosome biogenesis: PLK4, SAS6 and STIL. Mock-treated and *GL2* siRNA-transfected cells were used as negative controls. Untreated cells were also assessed.

3.1.1.1 Depletion of core centriolar proteins reduces centriole amplification in dysplasia cells

To test if depletion of PLK4, SAS6 or STIL leads to a reduction of CA in dysplasia cells, centrosome numbers were assessed in dysplasia cells after 3 and 4 days of siRNA transfection (Figure 3.1). To correctly assess centrosomes by immunofluorescence (IF), we labeled its two components: the PCM (with antibodies against pericentrin) and the centrioles (with antibodies against centrin). Centrosomes were considered when these two markers colocalized and, in this analysis, only interphase cells were analyzed. In interphase, cells in G1 normally have one centrosome (two centrioles) and cells in S phase or G2 already have two centrosomes (four centrioles). As cell cycle markers were not used, only cells with more than four centrioles were considered to have centriole amplification (Figure 3.1 A and D). Similar to what had been previously described for other cell lines[55,57,58], PLK4 and SAS6 depletion led to a reduction in CA when compared to the controls, in both CP-C and CP-D cell lines (Figure 3.1 B and E). Also, depletion of PLK4 or SAS6 led to an overall reduction of the number of centrioles found per cell (Figure 3.1 C and F). Seeing that centriole number reduction is achieved by dilution of existing centrioles through consecutive cell divisions, it is not surprising that the overall reduction of the number of cells with CA was accompanied by an increase in the population of cells with abnormally low numbers of centrioles (0 or 1 centrin foci; Figure 3.1 C and F). Interestingly, SAS6 depleted-cells appeared to exhibit a stronger effect in the reduction of CA when compared to PLK4 depletion. Surprisingly, however, STIL depletion did not appear to affect the incidence of CA and cells appeared to have a similar centriole number content to the control. Although the siRNA oligonucleotides against *STIL* have been successfully used in the lab to deplete STIL in other cell lines, a possible

explanation for this result could be that the siRNA against *STIL* was not efficient in these cells. We will therefore need to test for the efficiency of depletion of all the targeted molecules by analyzing their protein and/or mRNA levels by western blot and qRT-PCR, respectively. Nevertheless, these tests show that depletion of the core centriole biogenesis proteins PLK4 or SAS6 is able to reduce CA in dysplasia. Importantly, these tests also provide information regarding the timings of depletion so that we could get a good balance between efficiently reducing CA levels, without leading to a large number of cells with abnormally low numbers of centrioles (0 centrioles). This will be useful when performing the different migration and invasion assays.

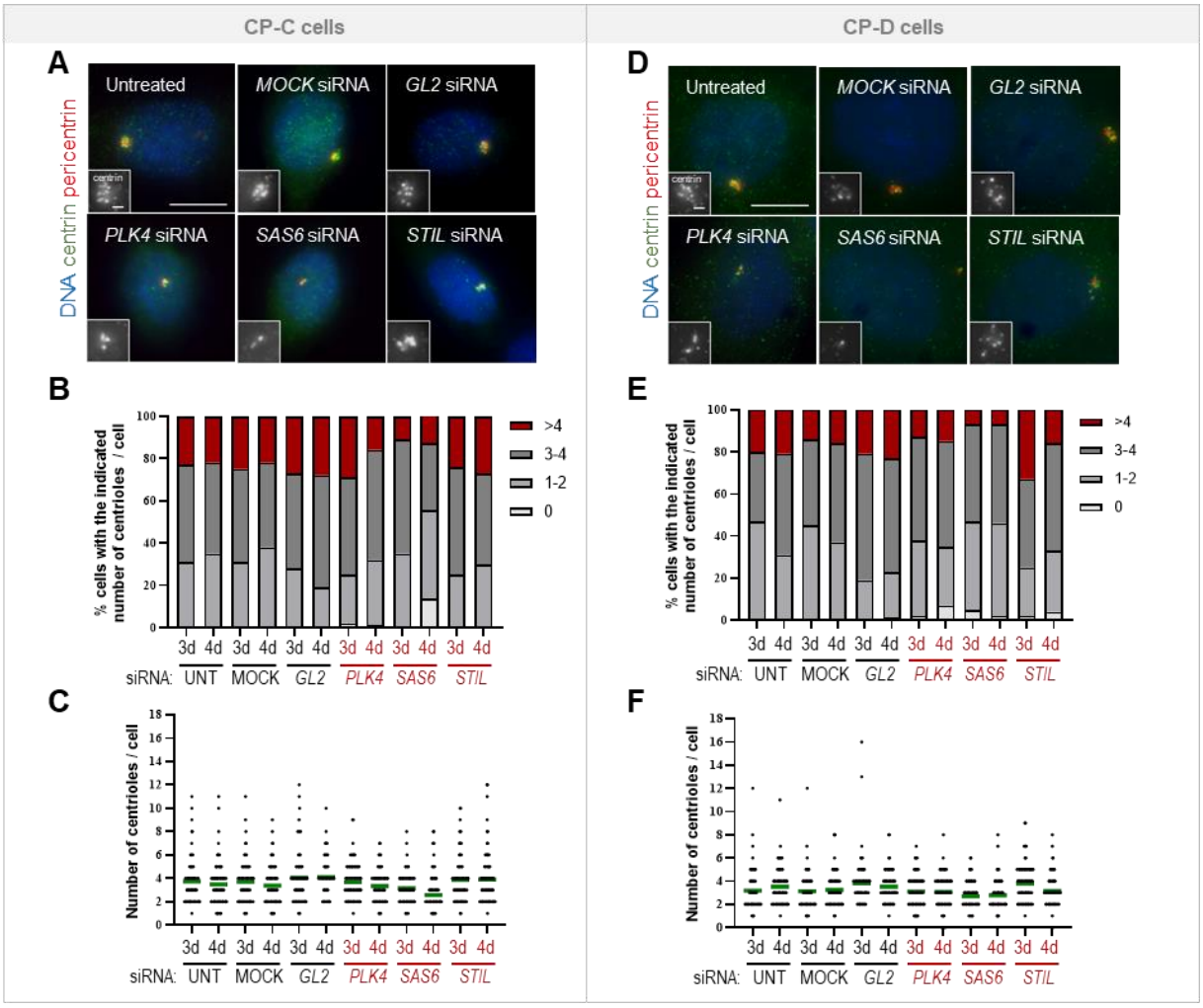

Figure 3.1 – Depletion of core centriole biogenesis proteins reduces CA in dysplasia cells. CP-B (A-C) and CP-D (D-F) dysplasia cells transfected with control (*GL2*) or *PLK4*, *SAS6* and *STIL* siRNA for 3 and 4 days were stained for PCM (pericentrin), centrioles (centrin) and DNA. Untreated and mock-treated cells were also analyzed. **(A and D)** Representative images of cells after 4 days of siRNA transfection. Insets show enlargements of centrioles. Scale bars: 10 µm (main images), 1 µm (insets). **(B and E)** Quantification of interphase cells with the indicated number of centrioles in each cell. **(C and F)** Number of centrioles in each cell. Green line indicates mean. (N=1; n=100 cells/condition).

3.1.1.2 2D migration and invasion assays did not reveal conclusive differences in the migration and invasive properties of dysplasia cells with reduced levels of CA

To assess if the observed reduction of CA in dysplasia leads to a reduction of the migratory and invasiveness capacity of these cells, we then performed 2D migration and invasion assays. Seeing that a reduction of CA in dysplasia was detected after 3 and 4 days of siRNA transfection, we decided to perform these migration and invasion assays after 3 days of transfection and analyze them 24h later (i.e. after 4 days of siRNA transfection). This would ensure that the cells would already have reduce CA

levels at the time these assays were initiated and that those lower levels were maintained throughout the time of the assays. Here, we tested this setup in CP-B (Figure 3.2 A) and CP-D cells (Figure 3.3 A).

As we had previously observed, there was a reduction of CA levels and an overall reduction of the number of centrioles per cell and CA levels upon PLK4 and SAS6 depletion in both CP-B (Figure 3.2 B and C; Figure S7.1 A and B) and CP-D cells (Figure 3.3 B; Figure S7.2 A and B), while STIL siRNA did not lead to any changes. However, the 2D migration and invasion assays performed were mostly inconclusive and suggest that further optimization of these assays may be needed. Regarding the wound healing assay, and despite our preliminary tests to determine the seeding density and time to achieve optimal cell confluence before removing the insert (see above in 'Material and Methods' for more details), the aimed confluency for CP-B cells was not observed at time zero because cells did not appear to attach properly. So, instead of having a directional migration towards the gap, a non-directional migration was also observed between the cell-free spaces (Figure S7.1 C), and the results were therefore inconclusive. As for CP-D cells, the wound healing assay showed that PLK4 depleted-cells appeared to close the gap faster than in other conditions, which were quite similar to the control (Figure 3.3 C). However, seeing that the cell confluence observed at time zero of the assay was not 100% optimal and cell-free spaces were still observed (Figure 3.3 C), these findings need to be interpreted with caution. In fact, the transwell migration assay did not reveal any significant differences between conditions in both CP-B (Figure 3.2 D) and CP-D (Figure 3.3 D) cells.

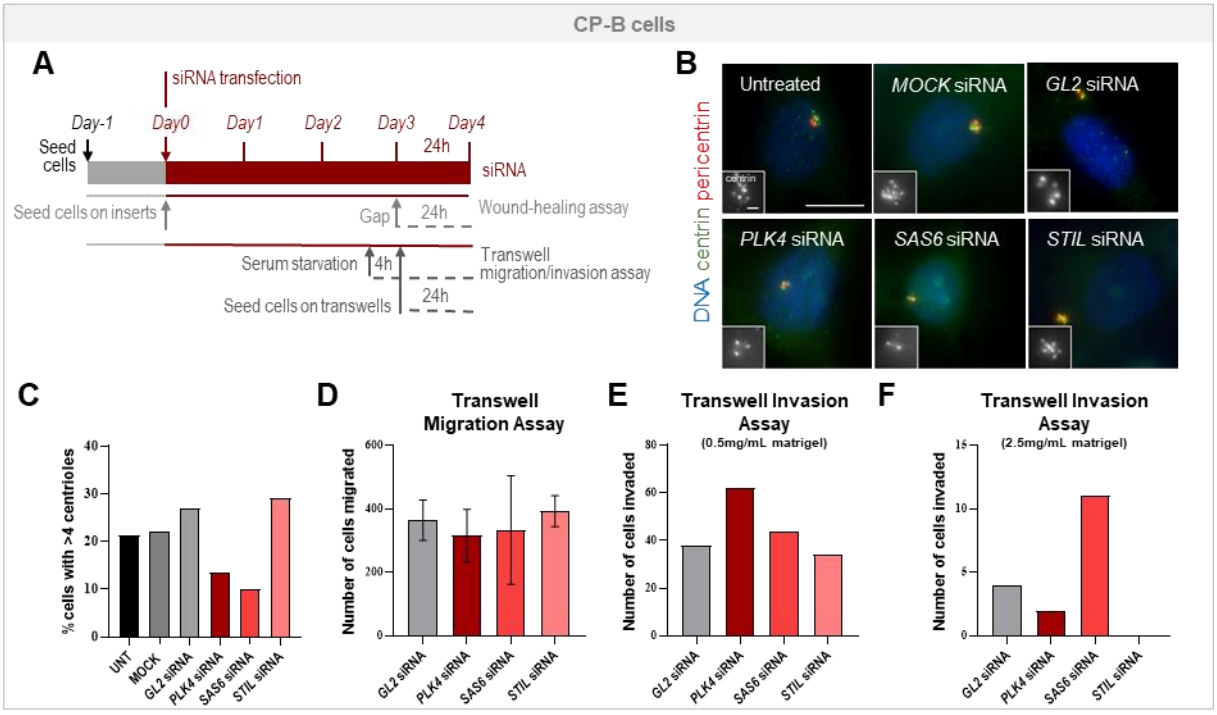

Figure 3.2 – Migration and invasion assays with CP-B cells with reduced CA by depleting core centriole protein by siRNA. Dysplasia CP-B cells transfected with control (*GL2*) or *PLK4*, *SAS6* and *STIL* siRNA for 3 days were submitted to migration and invasion assays (wound healing and transwell migration and invasion assays). **(A)** Scheme of the experimental design. **(B)** Representative images of cells after 4 days of siRNA. Insets show enlargements of centrioles. Scale bars: 10 µm (main images), 1 µm (insets). **(C)** Quantification of cells with centrosome amplification (>4 centrioles) after 4 days of siRNA transfection (N=1, n=100 cells/condition). **(D)** Number of cells migrated in a transwell migration assay. The results represent the mean of 2 technical replicates from the same experiment and the respective standard deviation. **(E-F)** Number of cells invaded in a transwell invasion assay with either 0.5 mg/mL (E) or 2.5 mg/mL (F) of matrigel

Finally, regarding the invasion transwell assays, cells were serum starved for 4h and we tested the capacity of cells to invade a matrix with different concentrations of matrigel, 0.5 or 2.5 mg/mL. Interestingly, although untreated CP-B cells appeared to invade better the matrix with a lower concentration of matrigel (Figure 3.2 E and F), CP-D cells appeared to have similar capacity to invade regardless the concentrations of matrigel (Figures 3.3 E and F). As for the effect of the different siRNA conditions, PLK4 depletion appeared to slightly increase the invasive capacity of CP-B cells (Figure 3.2 E), which was unexpected. Similarly, in a setting with a matrix with higher concentration of matrigel, SAS6-depleted CP-B cells appeared to be more invasive than control cells (Figure 3.2 F).

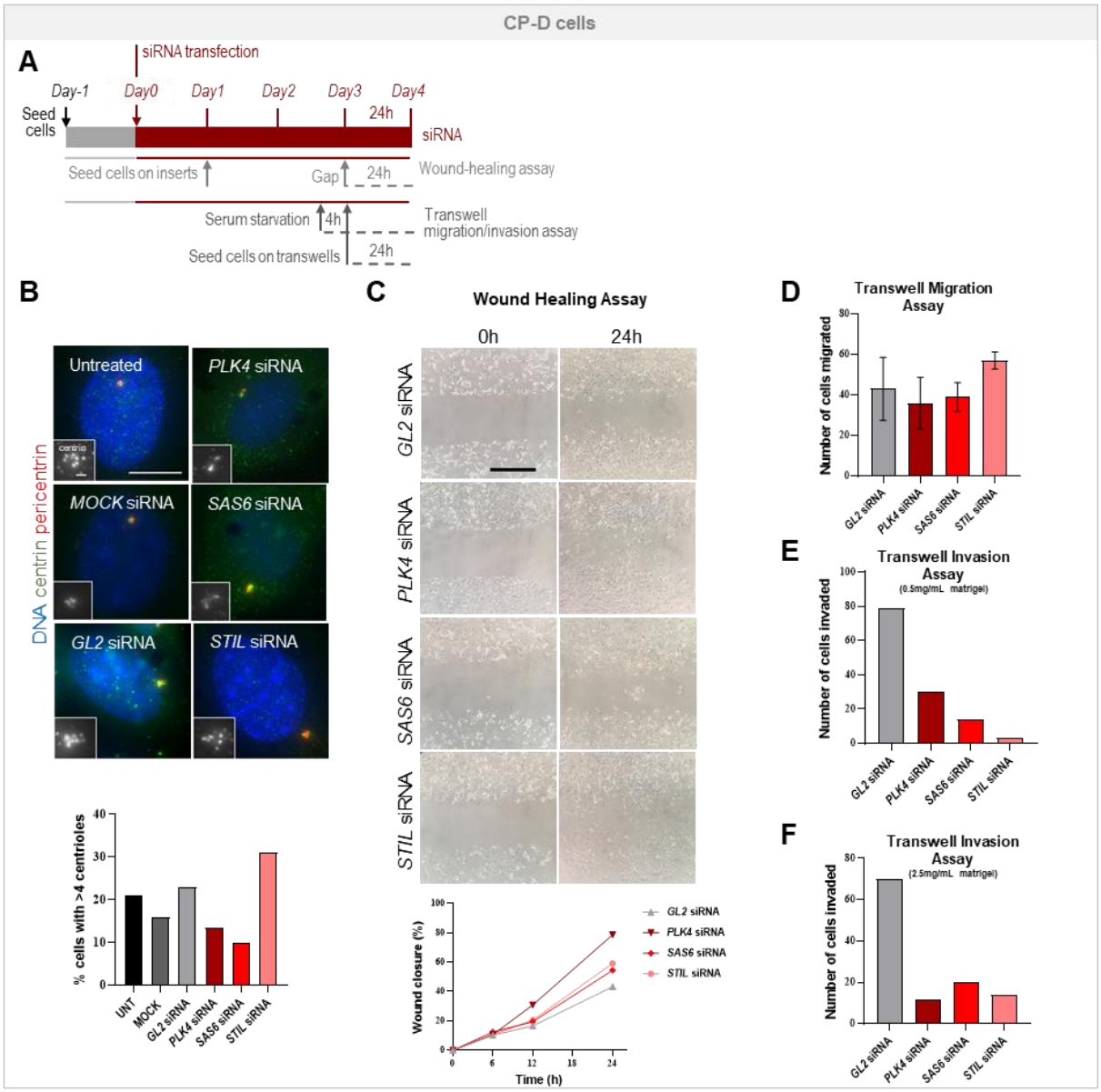

Figure 3.3 – Migration and invasion assays with CP-D cells with reduced CA by depleting core centriole protein by siRNA. Dysplasia CP-D cells transfected with control (*GL2*) or *PLK4*, *SAS6* and *STIL* siRNA were submitted to migration and invasion assays (wound healing and transwell migration and invasion assays). **(A)** Scheme of the experimental design. **(B)** Representative images of cells after 4 days of siRNA. Insets show enlargements of centrioles Scale bars: 10 µm (main images), 1 µm (insets), Histogram shows quantification of cells with centrosome amplification (>4 centrioles; N=1, n=100 cells/condition). **(C)** Bright-field microscopy images of wound closure at time zero (0h) and 24h after creating wound/gap (Scale bar: 0.5mm). Graph shows the percentage of the wound area closed by migrating cells at the indicated time points. Data points represent the mean of three measurements per condition. **(D)** Number of cells migrated in a transwell migration assay. The results represent the mean of 2 technical replicates from the same experiment and the respective standard deviation. **(E and F)** Number of cells invaded in a transwell invasion assay with either 0.5 mg/mL (E) or 2.5 mg/mL (F) of matrigel.

However, given the very low counts of cells invading in the control condition, we consider that this matrix concentration may not be ideal to test the invasiveness capacity of CP-B cells. In CP-D cells, all tested conditions (*PLK4*, *SAS6* and *STIL* siRNA) led to a significant reduction in their invasiveness capacity, regardless of their efficiency in reducing CA levels (Figure 3.3 E and F).

Overall, the results obtained in these tests with CP-B and CP-D cells suggest that some of the timings and conditions of these migration and invasion assays need to be further optimized. Here, we decided to focus on the CP-D cell line for this optimization (Figure 3.4 A). To achieve an optimal starting cell confluence in the wound healing assay, CP-D cells were seeded in the 2-well culture inserts right at the beginning of the transfection. For the transwell migration and invasion assays, cells were serum starved for 24h (instead of 4h, as previously done), more chemoattraction was added to the bottom chamber (10% FBS, instead of 5%), and standardized matrigel-coated inserts were used.

Consistent with what we had previously observed, depletion of PLK4 and SAS6 by siRNA in CP-D cells led to a reduction of CA levels (Figure 3.4 C) and overall number of centrioles per cell (Figure S7.3 A and B). However, and also as previously observed, depletion of STIL did not. A possible explanation for this unexpected result is that depletion of STIL did not affect CA. To confirm this, we assessed total protein levels by western blot (WB) (Figure 3.4 B). Indeed, while SAS6 protein levels were reduced upon siRNA transfection, STIL protein levels were unchanged. Surprisingly, STIL was upregulated upon PLK4 or SAS6 depletion. As for PLK4, given that protein levels are particularly difficult to assess by WB, we intend to confirm its depletion by assessing its mRNA levels by qRT-PCR. Moreover, seeing that STIL protein levels appeared to be unchanged upon its siRNA, but accumulated upon PLK4 or SAS6 depletion, it will be important to also assess its mRNA levels in the different conditions. Interestingly, analysis of the mRNA levels of both SAS6 and STIL by qRT-PCR throughout BE progression (Figure S7.4) revealed that the levels of SAS6 and STIL in dysplasia cells (CP-B and CP-C cells; CP-D cells were not analyzed) is higher than in metaplasia (BAR-T) or normal esophagus (EPC2) cells. These results suggest that STIL protein and/or its regulatory mechanisms, may be particularly deregulated in these cells, and further optimization of its depletion may be needed.

Despite efficient depletion of PLK4 and SAS6 and their resulting reduced CA levels, the wound healing assays revealed no differences in their migratory behavior when compared to the controls. (Figure 3.4 D and E). Seeing that the cell confluency at time zero was better achieved, when comparing with the previous test, these results suggest that reduction of CA does not affect the migratory behavior of dysplasia cells. As for the migration transwell assay, the results were puzzling and inconclusive, particularly given the variability observed within the technical replicates. Contrary to what we had observed in the previous tests, SAS6 depletion and STIL siRNA treatment appeared to increase the migration capacity of these cells (Figure 3.4 F). However, seeing the significant differences obtained between controls (untreated and *GL2* siRNA), these results need to be interpreted with caution and further biological replicates are needed to obtain conclusive results. Finally, regarding the invasion transwell assays, we found that depletion of PLK4 or SAS6 led to a reduction of the invasiveness capacity of CP-D cells, while *STIL*-siRNA treated cells were similar to the control (Figure 3.4 F). These results suggest that CA reduction hinders the invasiveness capacity of CP-D cells.

To assess if this reduction was due to changes in the mesenchymal state of these cells, we analyzed the protein levels of mesenchymal markers (fibronectin and vimentin) upon CA reduction (Figure 3.4 B) by WB. Surprisingly, we found that fibronectin appeared to be overexpressed upon SAS6 depletion and STIL siRNA treatment, and that vimentin was found to be upregulated upon PLK4 or SAS6 depletion (Figure 3.4 B).

Overall these tests indicate that these 2D migration and invasion assays may need further optimization (particularly the wound healing assay) and that several technical replicates should be performed to reduce the experimental variability obtained with these assays. Nevertheless, these tests confirmed that CA can be reduced in dysplasia through PLK4 or SAS6 depletion, and suggest that although CA may not contribute to the migratory capacity of dysplasia cells, it may contribute to their invasiveness potential.

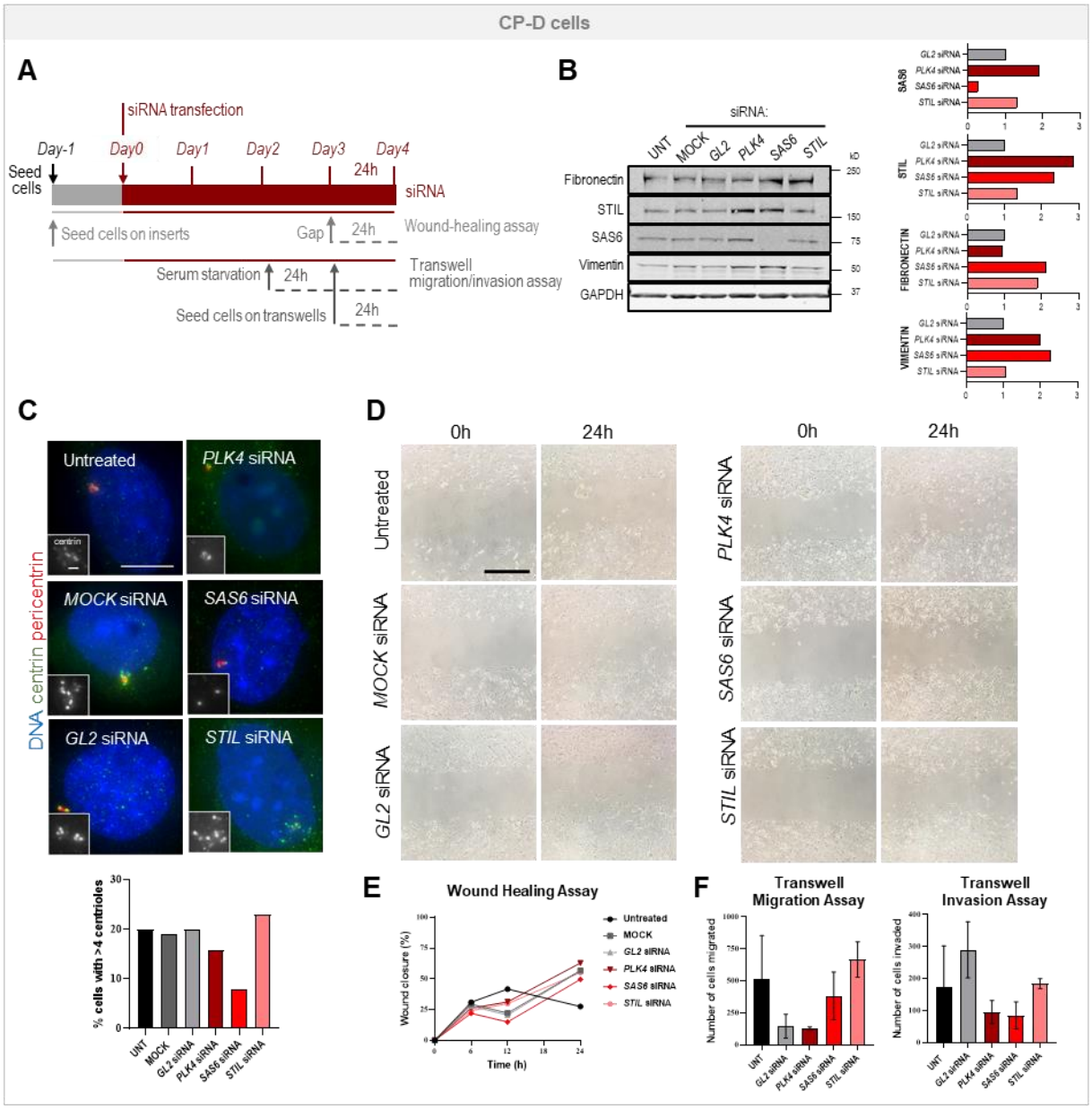

Figure 3.4 – Optimized migration and invasion assays with CP-D cells with reduced CA by depletion of core centriole biogenesis proteins by siRNA. Dysplasia CP-D cells transfected with control (*GL2*) or *PLK4*, *SAS6* and *STIL* siRNA were submitted to migration and invasion assays (wound healing and transwell migration and invasion assays). **(A)** Scheme of the experimental design. **(B)** Protein levels assessed by western blot and respective quantifications that were normalized to the *GL2* siRNA control. **(C)** Representative images of cells after 4 days of siRNA. Insets show enlargements of centrioles Scale bars: 10 µm (main images), 1 µm (insets). Histogram shows quantification of cells with centrosome amplification (>4 centrioles; N=1, n=100 cells/condition). **(D)** Bright-field microscopy images of wound closure at time zero (0h) and 24h after creating wound/gap (Scale bar: 0.5mm). **(E)** Percentage of the wound area closed by migrating cells at the indicated time points. Data points represent the mean of three measurements per condition. **(F)** Number of cells migrated and invaded in a transwell assay. The results represent the mean of 2 technical replicates from the same experiment and the respective standard deviation.

3.1.1.3 3D cell cultures showed a possible role of CA in the invasiveness capacity of dysplasia cells

To see if the reduction of CA leads to a reduction of the invasiveness capacity of dysplasia cells, transfected dysplasia cells were grown in a 3D matrix. If our hypothesis was correct, we expected to see a reduction in the number and/or size of invasive protrusions in cells depleted of PLK4 or SAS6. In this particular assay we also assessed the effect of depleting both PLK4 and SAS6 at the same time. With this, we wanted to check if this co-depletion led to an increased reduction of CA levels, and consequently further reduction of the invasiveness potential of dysplasia cells. Consistent with what had been previously observed with MCF10A cells with CA[29], previous tests from our lab had shown that the invasive behavior of dysplasia cells was only detected after 4 days in 3D cultures. Our preliminary tests using these 3D assays showed that seeding cells in 3D cultures on the same day as siRNA transfection was performed, did not reveal evident differences between conditions (data not shown). It is therefore possible that an effect in the invasiveness capacity may only be detected if depleted cells are grown in 3D cultures only after a significant CA reduction is achieved. Knowing this, cells were first transfected for 3 days and then re-transfected just before starting the 3D cultures, to try to ensure that CA was reduced at the time cells were cultured in 3D and that PLK4 and/or SAS6 depletion was maintained for the entire duration of the assay and thus avoiding a recovery in CA levels. We used CP-C cells for this assay (Figure 3.5 A).

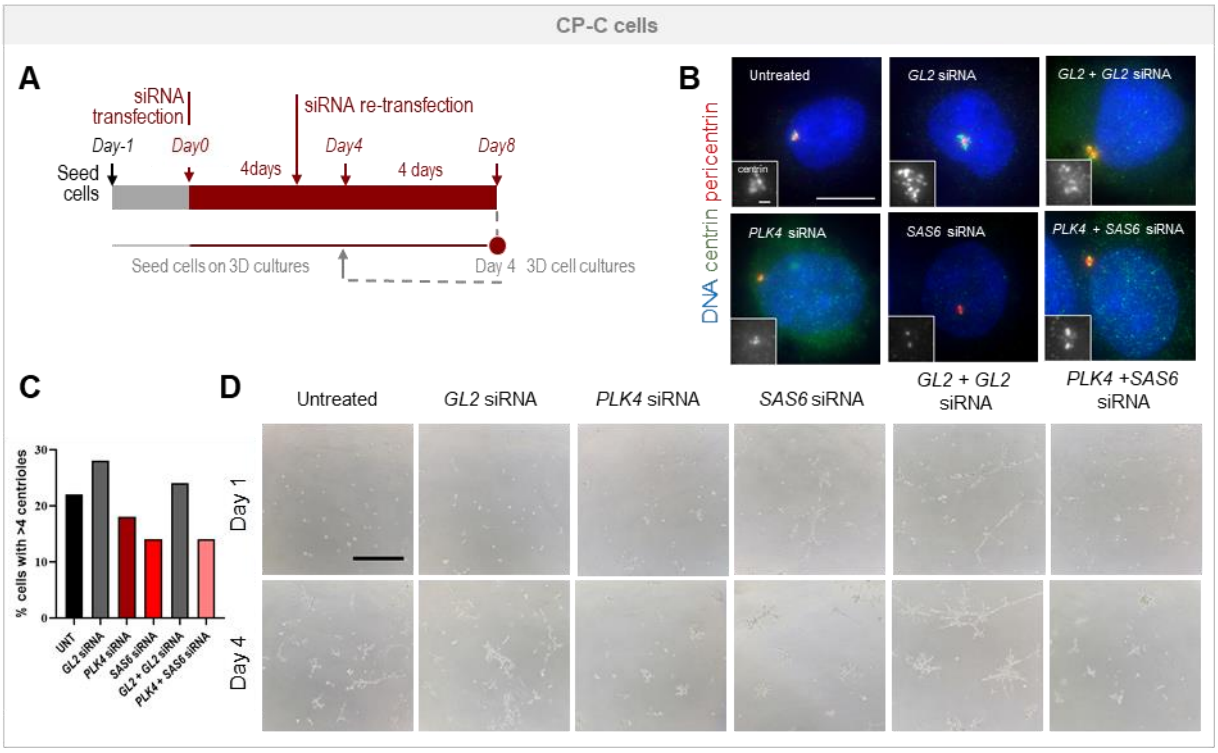

Figure 3.5 – Dysplasia cells with reduced CA through depletion of core centriole biogenesis proteins by siRNA showed a reduced invasiveness capacity in 3D cultures. Dysplasia CP-C cells transfected with control (*GL2*) or *PLK4*, *SAS6* siRNA and *PLK4+SAS6* co-depletion siRNA were submitted 3D cell cultures to assess for invasion. **(A)** Scheme of the experimental design. **(B)** Representative images of cells after 4 days of transfection (Day 0 of 3D cultures). Insets show enlargements of centrioles Scale bars: 10 µm (main images), 1 µm (insets) **(C)** Quantification of cells with centrosome amplification (>4 centrioles; N=1, n=100 cells/condition). **(D)** Bright-field microscopy images show cells grown in 3D cultures at Day 1 and Day 4 of the experiment. Scale bar: 0.5 mm.

As we had previously observed, there was a reduction of CA levels (Figures 3.5 B and C) and an overall reduction of the number of centrioles per cell (Figure S7.5 B and C) on the day 3D cultures were started (i.e. after 4 days of siRNA). The condition with a double depletion (PLK4+SAS6) showed the same outcome as the SAS6 individual depletion (Figure S7.5 B and C; Figure 3.5 B and C). Despite

the fact that the initial seeding was not optimal, because we had already an invasiveness phenotype after only one day in 3D, due to possible technical problems, the observation of cells through bright-field microscopy throughout the experiment showed a reduction in the number and size of the invasive protrusions in cells with PLK4, SAS6 and PLK4 + SAS6 double depletion after 4 days in these cultures (Figure 3.5 D).

3.1.2 Reducing centrosome amplification in dysplasia through chemical inhibition

In our second approach to reduce CA in dysplasia cells we used a validated selective chemical inhibitor against the activity of the key centriole duplication protein PLK4, called centrinone-B (here referred to has centrinone for simplicity)[57]. Cells treated with DMSO, the solvent of centrinone, were used as negative controls. Untreated cells were also analyzed.

3.1.2.1 Centrinone reduces centriole amplification in dysplasia cells

Treatment of HeLa cells (derived from human cervical cancer), with centrinone for 3 days has been previously shown to lead to an effective and drastic reduction in centrosome numbers, with 70% of cells exhibiting 0 centrosomes[57]. However, while the cells used in that study have a reported doubling time of 18h30[57], the dysplasia cell lines used here have a longer doubling time (34h, 58h and 39h for CP-B, CP-C and CP-D, respectively). By taking more time to divide, and since these treatment inhibits the formation of new centrioles but has not been described to affect the stability of already existing ones[57], cells will expectedly take more time to effectively reduce centriole numbers. Indeed, we observed only a mild reduction of the overall number of centrioles per cell with a slight increase in the population of cell with low numbers of centrioles, after 2 days of treatment (0 centrin foci; Figure 3.6 B and C). However, 3 days after the treatment, we observed a considerable increase of cells with CA, in spite of still having cells with abnormally low numbers of centrioles (0 centrin foci; Figure 3.6 B). These results suggest that inhibition of PLK4 with this inhibitor needs further optimization. A previous study using another PLK4 inhibitor, CFI-400945, showed that as PLK4 phosphorylates itself to promote its own degradation, an incomplete inhibition can actually lead to elevated PLK4 protein levels and subsequent higher levels of CA[59]. Although centrinone is a more selective PLK4 inhibitor than CFI-400945[57], it is conceivable that a similar effect could take place in suboptimal concentrations of centrinone.

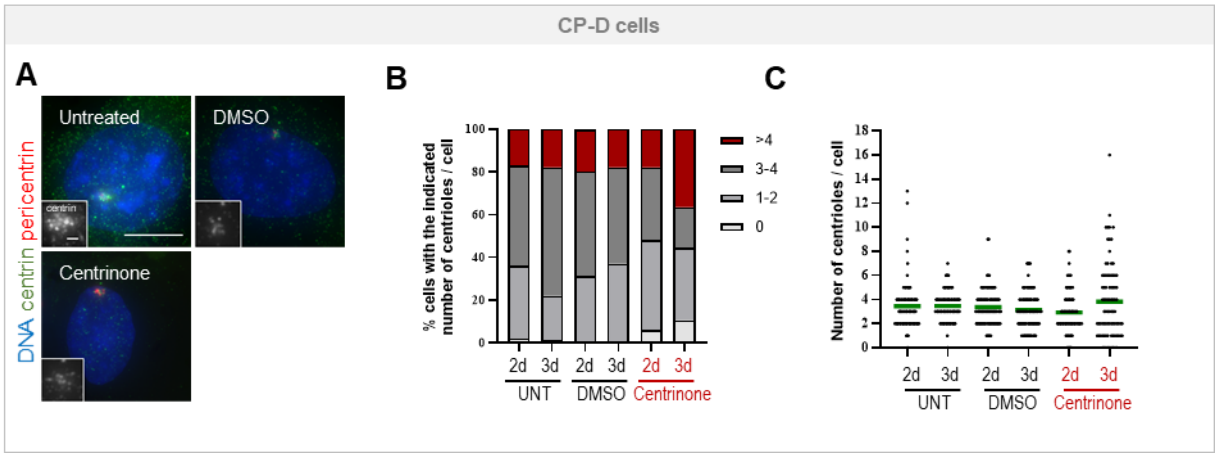

Figure 3.6 – Dysplasia cells exhibited increased CA levels after 3 days of continued treatment with centrinone. CP-D cells treated with centrinone for 2 and 3 days were stained for PCM (pericentrin), centrioles (centrin) and DNA. Untreated and DMSO treated cells were also analyzed. **(A)** Representative images of cells after 3 days of treatment. Insets show enlargements of centrioles. Scale bars: 10 µm (main images), 1 µm (insets). **(B)** Quantification of interphase cells with the indicated number of centrioles in each cell. **(C)** Number of centrioles in each cell. Green line indicates mean. (N=1; n=100 cells/condition).

We therefore posed the possibility that the inhibitor needed to be restored every 2 days to be effective in continuously inhibiting PLK4 activity. Indeed, our tests using CP-B (Figure 3.7 A-C) and CP-C (Figure 3.7 D-F) cells confirmed this hypothesis. Given the different reported doubling times for these cells lines (34h for CP-B and 58h for CP-C), we initially tested the effect of treating cells for either 6 days for CP-B and 8 days for CP-C cells. As CP-C cells take more time to divide, cells would expectedly take more time to effectively reduce centriole numbers. An effective reduction of CA and a percentage of approximately 35% of cells with 0 centrioles was found in both cell lines (Figure 3.7 B and E). With these tests, we optimized the centrinone treatment conditions and were able to understand the timings to use in the migration and invasion assays.

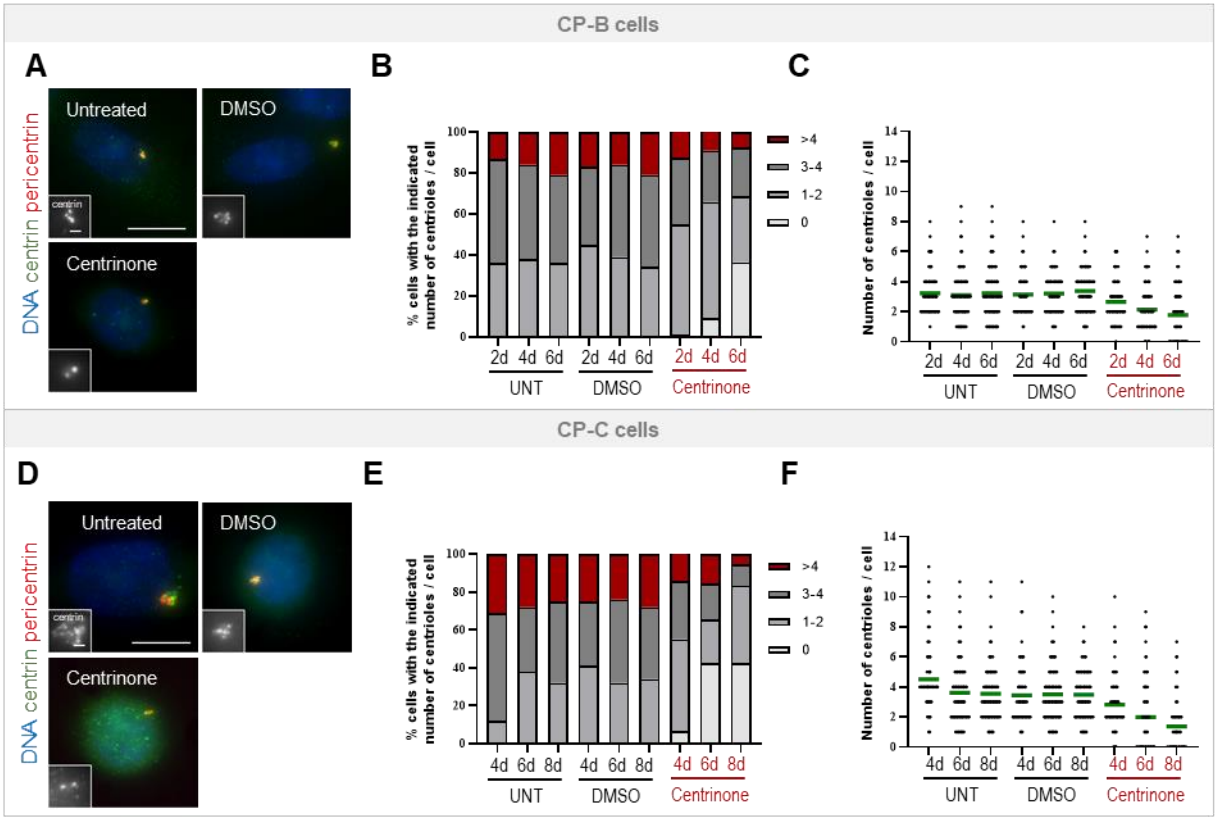

Figure 3.7 – Adding centrinone every 2 days leads to a reduction of CA levels in dysplasia. CP-B (A-C) and CP-C (D-F) dysplasia cells treated with centrinone were stained for PCM (pericentrin), centrioles (centrin) and DNA. Untreated and DMSO treated cells were also analyzed. **(A and D)** Representative images of cells after 6 and 8 days of treatment (A and D, respectively). Insets show enlargements of centrioles. Scale bars: 10 µm (main images), 1 µm (insets). **(B and E)** Quantification of interphase cells with the indicated number of centrioles in each cell. **(C and F)** Number of centrioles in each cell. Green line indicates mean. (N=1; n=100 cells/condition).

3.1.2.2 <u>2D migration and invasion assays did not show an impact in migration and invasive properties of dysplasia cells with reduced levels of CA, through a specific inhibitor</u>

As PLK4 inhibition was sufficient to reduce CA levels in dysplasia cells, we then tested if the reduction of CA in these cells lead to a reduction of the migratory and invasiveness capacity of these cells using 2D migration and invasion assays. Taking into account the CA reduction observed at the different timepoints analyzed (Figure 3.7), we decided to start these migration and invasion assays after

5 days of centrinone treatment and analyze them 24h later (i.e. after 6 days of treatment) (Figure 3.8 A). Here, we tested this setup in CP-C (Figure 3.8 B-D) and CP-D (Figure 3.8 E-G) cells.

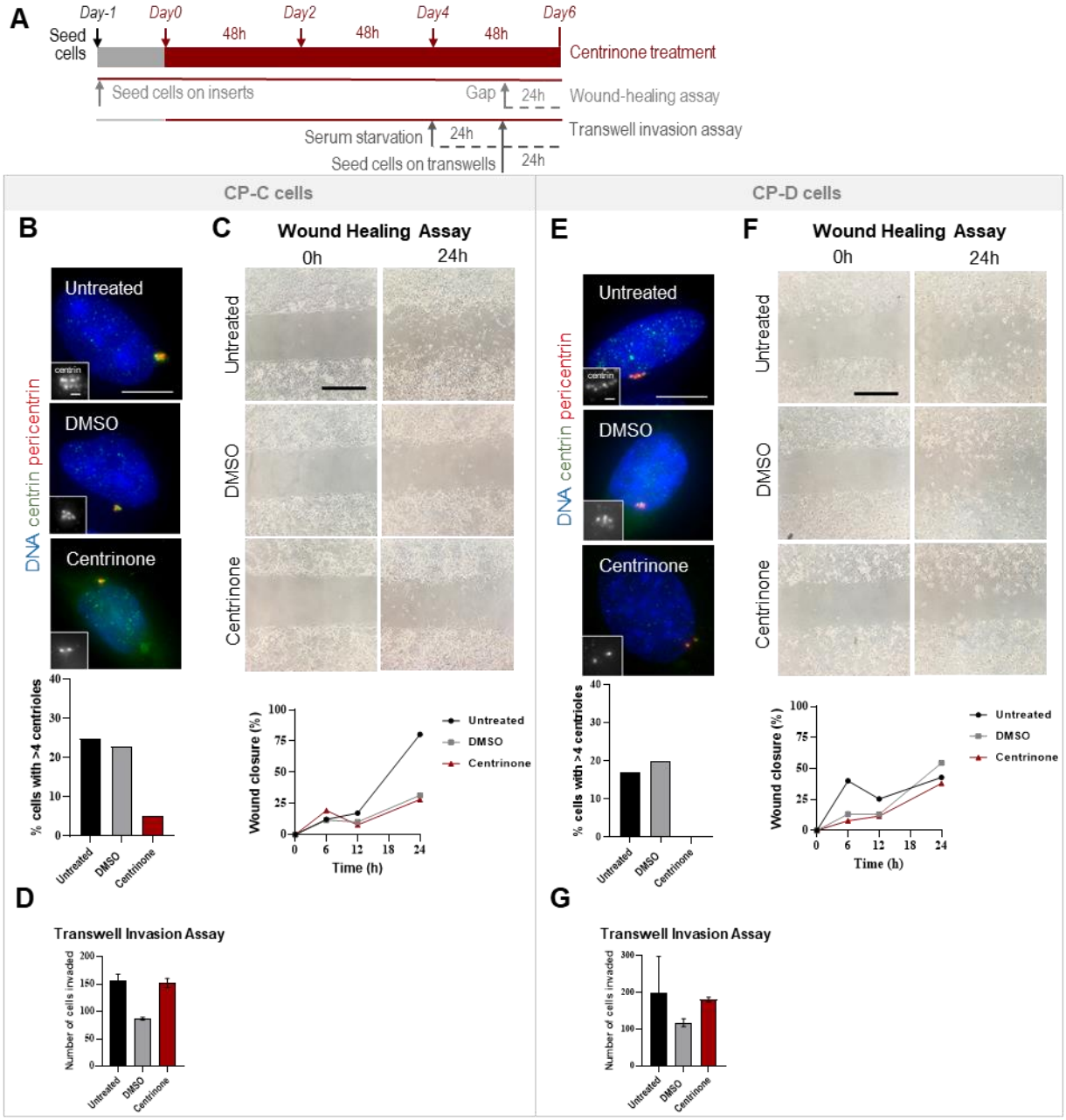

Figure 3.8 – Migration and invasion assays in dysplasia cells with reduced CA through PLK4 inhibition by centrinone. CP-C (B-D) and CP-D (E-G) dysplasia cells treated with centrinone were submitted to 2D migration and invasion assays (wound healing and transwell invasion assays). **(A)** Scheme of the experimental design. **(B and E)** Representative images of cells after 6 days of treatment. Insets show enlargements of centrioles Scale bars: 10 µm (main images). 1 µm (insets), Histogram shows quantification of cells with centrosome amplification (>4 centrioles; N=1, n=100 cells/condition). **(C and F)** Bright-field microscopy images of wound closure at time zero (0h) and 24h after creating wound/gap (Scale bar: 0.5mm). Graph shows the percentage of the wound area closed by migrating cells at the indicated time points. Data points represent the mean of three measurements per condition. **(D and G)** Number of cells invaded in a transwell assay. The results represent the mean of 2 technical replicates from the same experiment and the respective standard deviation.

In agreement with our previous results, centrinone treatment led to a reduction of CA levels (Figures 3.8 B and E) and an overall reduction of the number of centrioles per cell (Figure S7.6). However, and in agreement with what we had previously described in dysplasia cells with reduced CA

upon PLK4 or SAS6 depletion, the 2D migration assays did not revealed any differences in the migratory capacity in these cells. Regarding the wound healing assay, both cell lines achieved the optimal cell confluence at time zero and CP-C cell line actually appeared to be the better one to use for this type of assay (Figure 3.8 C). Unexpectedly, the two control conditions (untreated and DMSO-treated cells), in CP-C cells, had different outcomes, with DMSO showing similar migration rates to the centrinone-treated cells (Figure 3.8 C). CP-D cells exhibited the same migratory capacity in all conditions (Figure 3.8 F). Finally, regarding the invasion transwell assay, we found that both CP-C and CP-D cells treated with DMSO appeared to have a lower capacity of invading the matrix (Figure 3.8 D and G). These are unexpected and puzzling results. Surprisingly, centrione-treated cells exhibited and increased invasiveness capacity when compared to the DMSO-treated controls. These results suggest that reduction of CA by centrinone treatment may increase the invasiveness capability of these cells.

3.1.2.3 3D cell cultures showed a reduction in the invasiveness potential in dysplasia cells treated with the chemical inhibitor

We then assessed if the reduction of CA through centrinone inhibition leads to a reduction of the invasiveness capacity of dysplasia cells grown in a 3D matrix. If our hypothesis is correct, we expected to see a reduction in the number and/or size of invasive protrusions. Cells treated with centrinone for 5 days were then cultured in 3D for 4 and 7 days, while maintaining centrinone treatment (renewed every 2 days in the media) to ensure the continued inhibition of PLK4 and reduce CA levels. We used CP-B, CP-C and CP-D cells for this invasion assay (Figure 3.9 A). In agreement with our previous results, all cell lines exhibited a reduction of CA levels (Figure 3.9 C-E) and an overall reduction of the number of centrioles per cell (Figure S7.7), on the day that we cultured cells in 3D (i.e. after 5 days of centrinone treatment).

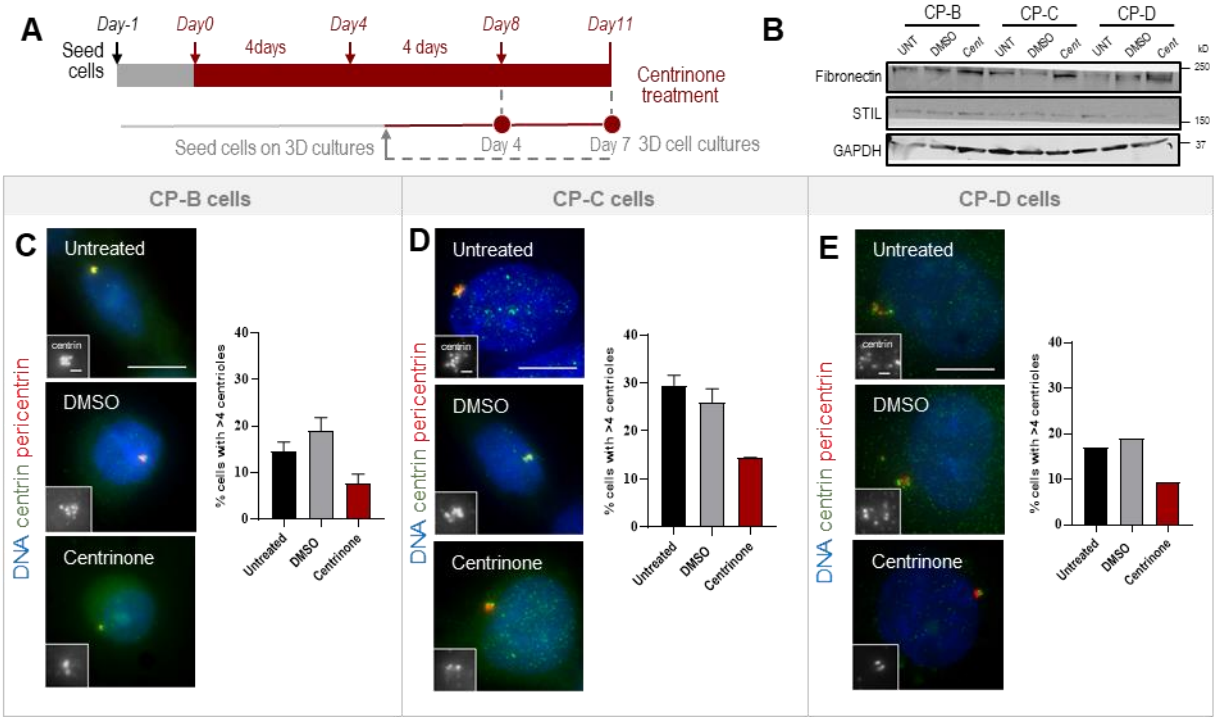

Figure 3.9 – Dysplasia cells used for 3D cell cultures showed a reduction of CA through PLK4 inhibition by centrinone. CP-B (C), CP-C (D) and CP-D (E) dysplasia cells treated with centrinone were grown in 3D cultures. **(A)** Scheme of the experimental design. **(B)** Protein levels assessed by western blot. **(C, D and E)** Representative images of cells after 5 days of treatment (Day 0 of 3D cultures). Insets show enlargements of centrioles Scale bars: 10 µm (main images), 1 µm (insets). Histogram shows quantification of cells with centrosome amplification (>4 centrioles). (C-D) N=2; n=100 cells/condition. Mean ± standard deviation. (E) N=1; n=100 cells/condition.

Also in agreement with what we had previously observed, untreated and DMSO-treated dysplasia cells started to exhibit protrusions after 4 days in 3D cultures, which became even more evident after 7 days (bright-field microscopy, Figure S7.8). In contrast, centrinone-treated cells exhibited an overall and clear reduction of number and/or size of protrusions (being clearer after 7 days) (Figure S7.8). Although all three dysplasia cell lines exhibited similar results, we found that centrinone-treated CP-D cells still exhibited some invasive features even after 7 days in 3D.

To better examine the invasive phenotype of these cultures, cells were stained with antibodies against α-tubulin to visualize the microtubule cytoskeleton, and therefore detect protrusions[29] (Figure 3.10 A, D and G). The organoids observed were divided into different classes that reflect the different degrees of complexity of cellular organization observed: single cells, sphere-like clusters of cells, and non-sphere-like clusters of cells. Additionally, to reflect the more or less invasive phenotype of the structures observed, each of these classes of organoids were further subdivided according to the absence or presence of invasive protrusions and/or more complex tubular structures[29,40].

As detected by bright-field microscopy analysis (Figure S7.8), all dysplasia cell lines in the control conditions (untreated and DMSO-treated) exhibited an invasive behavior that started to be detected at day 4 of 3D cultures and that was increasingly more evident with time in culture (Figure 3.10). Out of the three cell lines, CP-B control cells exhibited lower level of complexity in their organoids, particularly at day 4, where the majority of the organoids were single cell or sphere-like clusters, with or without protrusions. In contrast, cells treated with centrinone had more single cell and overall less invasive organoids than the controls (Figure 3.10 B). After 7 days of culture, while control cells exhibited all three classes of organoids, including non-sphere-like clusters with protrusions or tubules, cells treated with centrinone had a similar phenotype to that observed in control cells after 4 days (Figure 3.10 B). Importantly, we found that the number the number of cells within each organoid cluster in centrinone-treated cells was somewhat reduced after 4 days when compared to the controls (Figure 3.10 C). Moreover, while control cells formed complex organoids with high number of cells after 7 days, centrinone-treated cells formed organoids similar to that of 4 days of 3D cultures (Figure 3.10 C). Control CP-C cells exhibited a more complex and invasive phenotype than the CP-B cell line. After only 4 days in 3D cultures, it is already possible to distinguish all classes of organoids (Figure 3.10 E). In contrast, centrinone-treated CP-C cells after 4 days in 3D had more single cell and less invasive organoids than the controls. Similarly, while control CP-C cells exhibited organoids with increased complexity and invasiveness after 7 days, with the majority of the organoids forming non-spheroids clusters with high number of cells and complex tubules, centrinone-treated cells exhibited a significant reduction in organoids with tubules, and the presence of single cell or sphere-like clusters with lower numbers of cells (Figure 3.10 E and F). In fact, and similar to what was observed for CP-B cells, centrinone-treated CP-C cells at 7 days in 3D culture exhibited a phenotype similar to that observed to control cells after 4 days. Importantly, analysis of the cell cycle profile by flow cytometry, at the end of the assay, did not show any evident cell cycle arrest upon centrinone treatment in both CP-B and CP-C cells, suggesting that the reduced number of cells per cluster are not likely due to complete lack of proliferation in these cells (Figure S7.9). Finally, and as highlighted before, control CP-D cells exhibited the strongest invasive phenotype, with the majority of the organoids displaying highly complex non-spheroid clusters with branching tubules after only 4 days in 3D, and which became the dominant phenotype after 7 days (Figures 3.10 H and I). Although this strong invasive phenotype in 3D made the detection of differences upon treatment difficult, cells treated with the inhibitor showed an increase in the organoids without tubules, however maintaining protrusions (Figure 3.10 H). In this cell line it will be important to score the branching of tubules and measure the size of the protrusions to understand if the differences are more evident. Together these results show that, contrary to what was

observed in the 2D migration and invasion assays, reduction of CA levels leads to a reduced invasiveness capacity of dysplasia cells grown in 3D cultures, as it was already described in section 3.1.1.3 above.

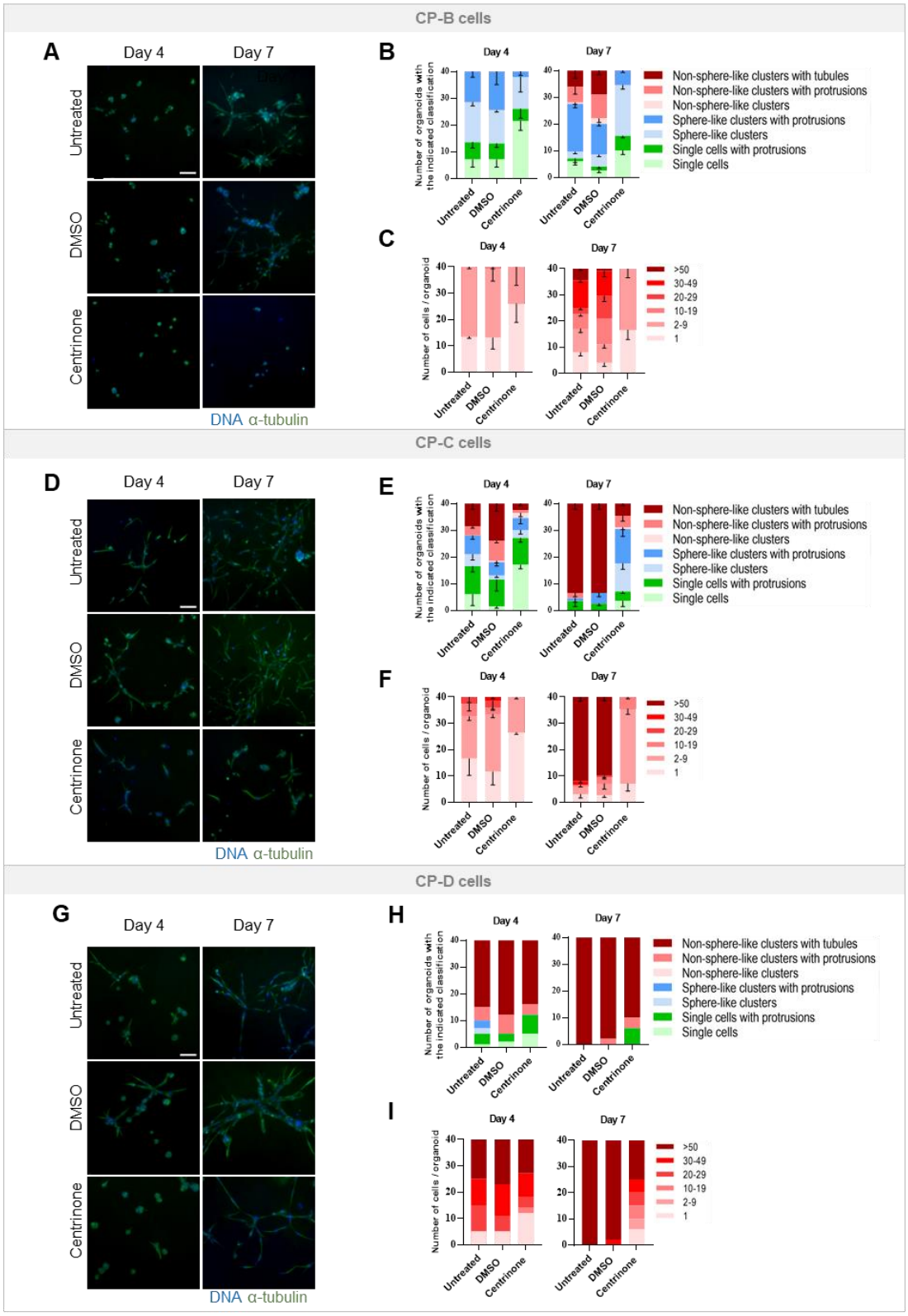

Figure 3.10 – Dysplasia cells with reduced CA through PLK4 inhibition had a reduction in the invasive structures in 3D cell cultures. CP-B (A-C), CP-C (D-E) and CP-D (G-I) dysplasia cells treated with centrinone for 5 days were cultured in 3D cell cultures. **(A, D and G)** Representative images of cells at Day 4 and Day 7, stained for microtubules (α-tubulin) and DNA. Scale bars: 100 µm **(B, E and H**) Number of organoids in the respective classes. (B-E) N=2; standard deviation. (H) N=1. **(C, F and I)** Number of cells per cluster. (C-F) N=2; standard deviation. (I) N=1.

To determine if the observed changes in dysplasia invasiveness potential upon CA reduction could be related to changes in the mesenchymal state of these cells, we assessed the total protein levels of mesenchymal and epithelial markers by WB (Figure 3.9 B). Notably, and similar to what we observed upon SAS6 and STIL siRNA treatment, there was an increase in fibronectin levels upon centrinone treatment in both cell lines. In the future it will be important to repeat these analyses to confirm any changes in the mesenchymal phenotype of these cells upon CA reduction.

3.2 The impact of increasing centrosome amplification in the migratory and invasiveness capacity of metaplasia cells

To understand the role of CA in promoting cell invasion in BE progression, it was equally important to understand if an increase in CA levels in metaplasia cells is sufficient to promote their invasive potential. For this, we used metaplasia cells (BAR-T) derived from a patient with non-dysplastic Barrett's esophagus[49,60] and where CA levels were found to be very low[49]. Once the conditions of increasing CA levels were optimized, we then performed 3D cultures to assess for changes in invasion.

3.2.1 Increasing centriole numbers in metaplasia by depleting p53 through siRNA transfection

Previous work from our lab had shown that depletion of the tumor suppressor p53 in metaplasia for 3 days was sufficient to increase the incidence of CA to similar levels detected in dysplasia[49]. We therefore decided to transfect metaplasia cells with specific siRNA oligonucleotides to reduce the expression of p53, and consequently increase CA levels in these cells. Mock-treated and *GL2* siRNA-transfected cells were used as negative controls. Untreated cells were also assessed.

3.2.1.1 Depletion of p53 increases the centrosome amplification levels, in metaplasia cells

To confirm that depletion of p53 leads to an increase of CA, centrosome numbers were assessed in metaplasia cells. Previous work has shown that MCF10A cells with CA exhibited invasive protrusions after 4 days in 3D cultures[29]. We therefore wanted to ensure that metaplasia would not only have such increased CA at the time these cultures were initiated, but also that those increased levels would be maintained throughout a 4-day 3D assay. To do this, we first transfected cells for 3 days and then re-transfected just before starting the 3D cultures to ensure that CA was increased at the time cells were cultured in 3D and that p53 depletion was maintained for the entire duration of the assay and thus avoiding a potential recovery in CA levels (Figure 3.11 A). To exclude potential off-target effects of the siRNA, we used 3 different siRNAs against TP53, all previously shown to lead to increased CA in metaplasia cells[49]. As previously described, p53 depletion led to an increase CA levels (Figure 3.11 B and C) and in the overall number of centrioles per cell (Figure S7.10 A and B) in all conditions where p53 was depleted.

3.2.1.2 3D cultures suggest that centrosome amplification is not sufficient to induce invasiveness in metaplasia cells

To see if the increase of CA leads to the acquisition of invasive capacity properties in metaplasia cells, transfected metaplasia cells with increased CA were cultured in 3D (i.e. 4 days of siRNA). As mentioned above, preliminary results from our lab had shown that metaplasia cells grow as contained clusters of cells (similar to untreated MCF10A cells[29]) in 3D cultures. If our hypothesis was correct, we expected to see the formation of invasive protrusions in the organoids formed by cells depleted of p53. The observation of cells through bright-field microscopy throughout the experiment did not show any

differences between control cells and cells with increased CA (Figure 3.11 D). These results suggest that the increase of CA through p53 depletion is not sufficient to induce invasiveness in metaplasia cells. However, as protrusions formed may be small, detailed analysis by IF to analyze the MT network (as done for dysplasia cell lines grown in 3D cultures) must be performed. Moreover, it will also be important to check the effect of CA increase in these cells after longer periods in 3D cultures (e.g. 7 days). To avoid the technical challenges of re-transfecting cells in this context to ensure p53 depletion and consequently increase CA, we will test if using a specific inhibitor against p53 is also effective in inducing CA in metaplasia.

To assess for any alterations in the epithelial state of these cells, we checked protein levels of mesenchymal markers by WB (Figure S7.10 C). Although these results suggest there may be a decrease in the fibronectin levels, upon p53 depletion, further tests should be done.

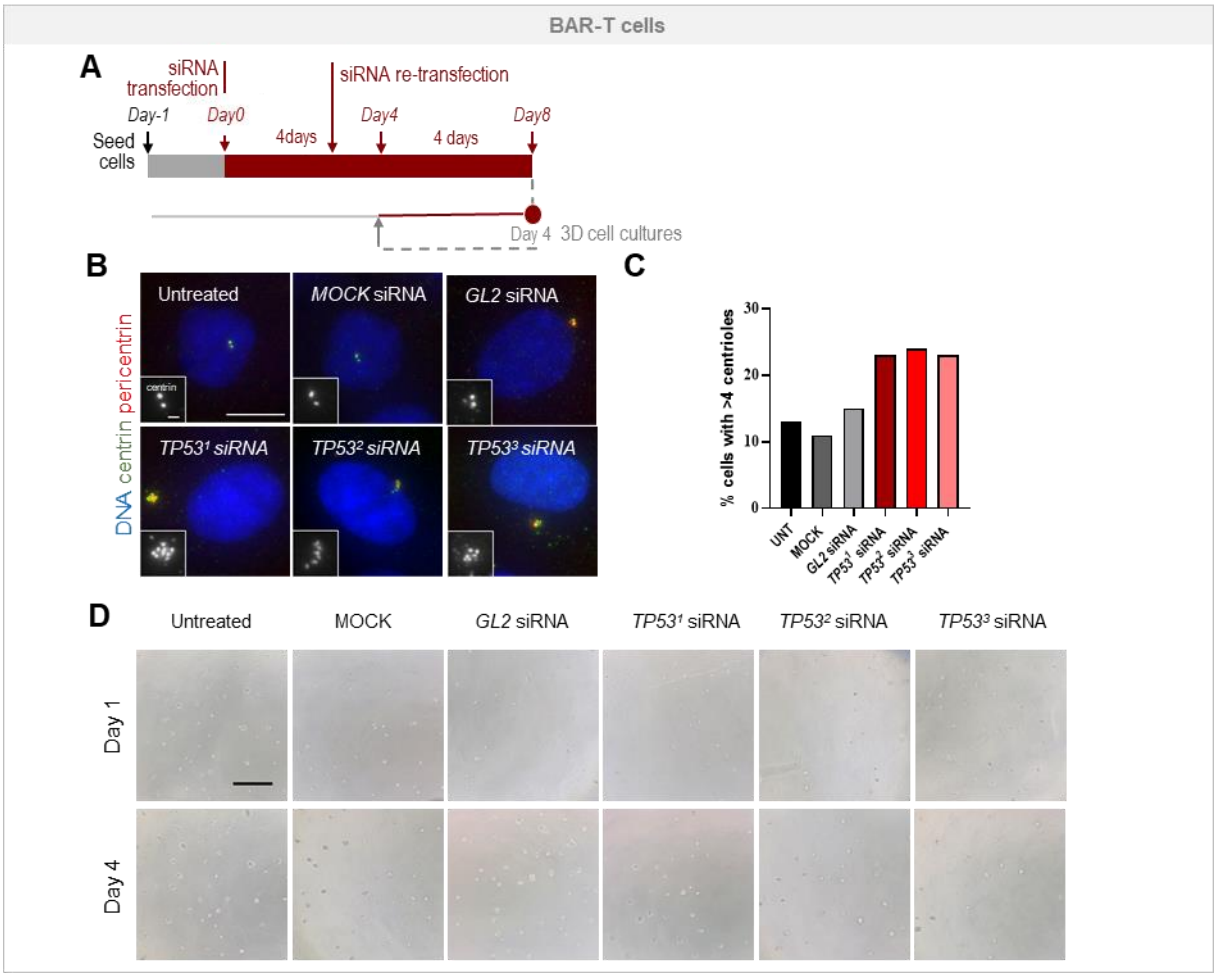

Figure 3.11 – Metaplasia cells with increased CA did not show differences in the invasiveness capacity in 3D cultures. BAR-T metaplasia cells transfected with control (*GL2)* or *TP53* siRNA were grown in 3D cultures. **(A)** Scheme of the experimental design. **(B)** Representative images of cells after 4 days of transfection (Day 0 of 3D cultures). Insets show enlargements of centrioles. Scale bars: 10 µm (main images), 1 µm (insets). **(C)** Quantification of cells with centriole amplification (>4 centrioles; N=1, n=100) **(D)** Bright-field microscopy images show cells grown in 3D cultures at Day 1 and Day 4 of the experiment. Scale bar: 0.5 mm.

4. DISCUSSION

Using BE as a human cancer model to study CA throughout malignant transformation, our lab as previously shown that CA arises as early as the premalignant condition and that its incidence increases upon neoplastic progression, suggesting it may promote tumor initiation[49]. Particularly, as the levels of CA significantly increase from metaplasia to dysplasia transition, it is possible that CA may contribute to BE progression by promoting the acquisition of malignant properties. Importantly, seeing that dysplasia cells have an invasiveness potential that metaplasia cells do not have[54], we hypothesized that CA could contribute to the invasiveness capability in BE progression. Knowing that metaplasia cells have low levels of CA, increasing these levels could lead to the acquisition of neoplastic characteristics, such as migration and invasion. On the other hand, as dysplasia cells have high levels of CA, reducing this amplification could reduce the capacity of cells to migrate and invade.

Here, we first asked if reduction of CA in dysplasia was sufficient to reduce the invasiveness capacity of dysplasia cells. Taking advantage of the unique panel of cell lines representing all stages of disease progression, we used three available cell lines derived from high-grade dysplasia samples from three different patients[49,56]. By studying the impact of CA in all three distinct representative cell lines, we will be able to determine the consistency or variability of the role of centrosome abnormalities in cancer progression, and thus determine the potential effects of inter-patient tumor heterogeneity, an important challenge for the design of effective clinical tools. To reduce CA in these cells we used two different approaches to affect key molecules of the centriole duplication machinery and thus reduce centriole numbers: depletion of PLK4, SAS6 or STIL by siRNA or inhibition of PLK4 activity through its selective inhibitor centrinone. Both approaches have been previously shown to be effective in reducing centriole numbers in other cell lines[57,61]. However, there are important differences between the approaches that need to be considered. On one hand, as the siRNA acts at the mRNA level, the effects at the protein level may take some time to be detected. Moreover, to ensure the continued silencing of the targeted protein, re-transfection of siRNA is needed after 3 or 4 days, which may represent a technical challenge in some contexts. On the other hand, centrinone treatment is technically more straightforward, as it can be added directly to the media, and since it acts directly on the protein's activity, its effects may be more quickly detected. It also has the advantage that it could be more easily translated into the clinic. Nevertheless, by allowing us to reduce CA by targeting different molecules, the siRNA approach allowed us to confirm that the potential effect in the invasiveness capacity of dysplasia cells is a direct consequence of the overall CA reduction, and not solely due to interfering with a specific molecule alone, such as PLK4. Here, we showed that both approaches were successful in reducing centriole numbers. Unexpectedly, however, we found that *STIL* siRNA did not lead to a reduction in CA, likely due to the inefficient reduction in its protein levels despite using siRNA oligonucleotides that had been previously validated in other cell lines in our lab. Interestingly, analysis of mRNA levels of STIL in cell lines from BE progression by qRT-PCR revealed that STIL appears to be significantly upregulated in dysplasia. This suggests that either the overexpression or posttranslational modifications / regulatory mechanisms that promote its stability may hinder its efficient depletion by siRNA in dysplasia. As expected, however, centrinone treatment appeared to lead to a faster and stronger reduction in CA levels than depletion of PLK4 by siRNA. As the main centriole duplication molecule, PLK4 is the most commonly manipulated molecule to increase/decrease centriole numbers[57,58]. Being upstream of both STIL and SAS6 in the duplication pathway, its depletion was expected to have the greatest impact in centriole numbers. However, SAS6 depletion appeared to lead to a stronger reduction in CA than PLK4 depletion. It will therefore be important to assess levels of all these proteins in BE progression. Notably, we also found that PLK4 siRNA led to an increase in the

protein levels of both SAS6 and STIL. To our knowledge no such effect has been previously reported and although we still do not know how to explain such changes, the upregulation of SAS6 and STIL upon PLK4 depletion may play some role in counteracting the efficient reduction in CA upon its depletion.

To assess the effects of reducing CA (by either siRNA or chemical inhibition) in dysplasia cells in their migratory and invasiveness potential, we then performed several classic 2D migration and invasion assays, as well as more complex 3D cultures to assess invasion. By testing cellular behavior in different setups and contexts, we aimed to have a more robust understanding of the potential effects of CA. However, technical challenges that demanded some optimization in the setup of the classic 2D migration and invasion assays rendered some of the results obtained inconclusive. For example, in the classic wound healing assay cells need to be confluent at the starting point, when the gap (i.e. wound) between cells is created, to make sure a directional migration towards the gap is observed. Despite several changes in the experimental setup to ensure such ideal starting conditions, this was difficult to obtain and indeed one of the cell lines (CP-B) did not attach and so we could not assess their behavior using this assay. To solve this problem, coating these cells probably will help with the attachment in future experiments. While such technical difficulties did not allow us to get robust results from several biological replicates of each experiment, the preliminary results obtained, using both wound healing assays and 2D transwell migration assays, suggest that CA reduction in dysplasia cells does not affect their migratory behavior. Although these results need to be confirmed by repeating these experiments in the optimized conditions, they are not consistent with findings from other studies. Indeed, previous studies in neuroblastoma tissue, colorectal cancer cell lines and mice with induced tumors in liver and lung, adressed the effect of PLK4 in migration using these specific directional migration assays, and all concluded that downregulation of PLK4 resulted in reduced directional migration[37,38,62,63]. However, and despite the known effect of PLK4 depletion in centriole numbers[57,58], they did not report any reduction in the number of centrioles. An interesting study highlighted an important role for the CEP85–STIL complex in modulating PLK4-driven cancer cell migration, as downregulation of STIL by siRNA reduced cell migration in wound healing assays[64]. Seeing that we could not test the effect of STIL depletion in our cells, as STIL appeared to be stable in these cells, and that STIL appeared to be overexpressed upon PLK4 or SAS6 depletion, in the future it will be important to study the importance of this protein and its interactions in dysplasia cell migration. The invasiveness potential of dysplasia cells has been previously demonstrated using transwell assays where cells with such capacity can cross a membrane coated with a matrix of matrigel into a lower chamber[54]. Importantly, previous studies using this type of assay showed that downregulation of PLK4 in neuroblastoma tissure and cancer cell lines resulted in less cells invading into the lower chamber[38,61]. We therefore expected that reduction of CA in dysplasia cells, using either the siRNA or inhibitor approaches, would lead their decreased capacity to cross the membrane. However, the results obtained here with these approaches were contradictory. Taking into account only the optimized experiments, we found that while PLK4 and SAS6 depletion resulted in less invasiveness in CP-D cells, just like it was expected and previously described for other cell types[38,61], centrinone-treated cells exhibited an increased invasiveness capacity when compared to the DMSO-treated control cells. Surprisingly, DMSO-treated cells appeared to be less invasive than their untreated counterparts. However, seeing that these optimized experiments were only performed once, and the variability observed between the technical replicates, these results need to be interpreted with caution until more biological replicates of the experiments are performed.

The invasiveness potential upon CA reduction in dysplasia cells was also assessed using more complex 3D cultures. Here, we found that reduction of CA levels with either the PLK4 inhibitor or depletion of PLK4 or SAS6 through siRNA, led to a decreased invasiveness capacity of all three

dysplasia cell lines, with cells showing an overall reduction of their invasive protrusions, just like we hypothesized. We also noted that the organoids formed were less complex, with less cells per organoid. This observation suggests that protrusions may only form with a higher number of cells per cluster and/or that cells with reduced CA are proliferating less. Previous work showed that cells treated with centrinone continued to proliferate at a slower rate, but that G1/S and G2 durations were not substantially different in centrosome-less cells compared with controls[57]. This was consistent with our results, but further analysis should be done. Centrinone treatment was also shown to increase the frequency of mitotic errors that led to cell death[57]. Although no significant cell death was observed in these cells in culture, further detailed assays should be performed to exclude this effect.

Several studies have investigated the possible mechanisms underlying the role of CA in migration and invasion. One mechanism through which CA could be affecting invasion is through the activation of Rac1, a small GTPase strongly associated with oncogenic signaling and with the induction of invasiveness and metastasis[65]. It was shown that CA-mediated activation of Rac1 in MCF10A cells leads to their invasive behavior in 3D cultures[29]. Cell migration involves a complex, multistep process that leads to the actin-driven movement of cells on or through the tissues of the body. A recent study has suggested that PLK4 can control cancer cell migration and invasion through the regulation of the actin cytoskeleton[61]. PLK4 interacts with the Arp2/3 complex, enhancing lamellipodia formation and cell migration. The Arp2/3 complex is the only molecular machine that generates branched actin networks[66]. Altered expression of one or more of the seven Arp2/3 complex subunits has been shown in several types of human epithelial malignancy[66,67]. To understand the mechanisms by which CA contributes to the invasiveness potential of dysplasia cells, it will be important in the future to check their effect in the actin cytoskeleton and/or Rac1 activity. During cancer progression, tumor cells go through a process called epithelial to mesenchymal transition (EMT), characterized by loss of epithelial characteristics and the gain of mesenchymal characteristics, that will lead to capability of cells to migrate and invade other tissues and lead to the metastatic process[31,33,68]. To understand if observed effects in dysplasia invasiveness capacity correlate with the differential overall expression of these markers, we checked mesenchymal markers upon CA reduction. Previous studies showed that downregulation of PLK4 lead to increased expression level of epithelial markers and a decrease in mesenchymal markers in shPLK4-depleted neuroblastoma cells and in colorectal cancer cells[37,38], suggesting that PLK4 mediated EMT in these cells. On the other hand, induction of CA in MCF10A cells did promote EMT changes[29,40]. Surprisingly, however, our results showed that reduction of CA in dysplasia was accompanied by an unexpected increase in the mesenchymal markers vimentin (upon PLK4 and SAS6 depletion) and fibronectin (upon SAS6 depletion and inhibition of PLK4 activity). Fibronectin is known to be upregulated in late stages of metastatic tumors[69]. Fibronectin secreted into the extracellular matrix plays important roles in cell migration, invasion, angiogenesis, and tumor cell growth[69,71]. Indeed, disruption of fibronectin secretion in prostate cancer cells was found to lead to its accumulation in cytosolic vesicles called endosomes and resulted in the reduced invasion capacity of these cells[72]. Interestingly, centrosomes have been shown to play an important role in the endosome recycling pathway[73]. We therefore hypothesize that defective fibronectin trafficking into the extracellular matrix may play an important role in the reduced invasiveness capacity of dysplasia cells upon CA reduction. Analysis of fibronectin by IF and of its secretion by ELISA in dysplasia cells before and after CA reduction will be important to test this hypothesis.

Here, we also tested if the increase in CA levels early in metaplasia would be sufficient to lead to the acquisition of an invasiveness potential at this stage. To increase CA levels, we aimed to test two different strategies: overexpression of PLK4 or SAS6, or p53 depletion by siRNA. While technical problems with plasmid transfection precluded the analysis of the first strategy, we were able to

successfully increase CA levels in metaplasia with all the siRNAs targeting p53, just as previously described[49]. However, and unlike what was previously found for breast epithelial cells with increased CA[29], metaplasia cells with increased CA grown in 3D cultures did not apparently exhibit the formation of protrusions, indicative of an invasiveness potential. Still, these experiments need to be further analyzed and repeated, other strategies to induce CA in metaplasia need to be tested, and different assays to assess migration and invasion performed to confirm these results. Nevertheless, these observations suggest that CA may not be sufficient to induce invasion in metaplasia cells and that other molecular changes may be needed for cells to acquire the invasiveness potential present at later stages.

5. CONCLUSION AND FUTURE PERSPECTIVES

With this work, we concluded that CA promotes the acquisition of the invasive capacity in dysplasia cells. Importantly, our work also provided important clues into possible new mechanisms by which centrosome deregulation may contribute to tumor progression that will be explored in the future. By contributing to our understanding of the impact of CA in the acquisition of malignant properties in BE progression and their underlying mechanisms, our work will help determine the effectiveness of targeting those abnormalities, such as using specific chemical inhibitors, in preventing cancer progression. Importantly, by demonstrating a role for CA in BE progression, this work also supports the use of CA as a potential biomarker that would help determine the patients with BE with increased risk of progressing to the next stages of disease. This is particularly relevant for the management of BE, as new screening tools are needed. Finally, as CA is present in most human tumors, perhaps this knowledge could be transposed to other cancers, or even other diseases in which centrosome deregulation is prevalent such as ciliopathies and microcephaly

6. REFERENCES

1. Godinho, S. A. & Pellman, D. Causes and consequences of centrosome abnormalities in cancer. *Philos. Trans. R. Soc. B Biol. Sci.* **369**, (2014). doi:10.1098/rstb.2013.0467

2. Fletcher, D. A. & Mullins, R. D. Cell mechanics and the cytoskeleton. **463**, 485–492 (2010). doi:10.1038/nature08908

3. Joukov & De Nicolo. The Centrosome and the Primary Cilium: The Yin and Yang of a Hybrid Organelle. *Cells* **8**, 701 (2019). doi:10.3390/cells8070701

4. Sanchez, A. D. & Feldman, J. L. Microtubule-organizing centers : from the centrosome to. *Curr. Opin. Cell Biol.* **44**, 93–101. doi:10.1016/j.ceb.2016.09.003

5. Scheer, U. Historical roots of centrosome research: Discovery of Boveri's microscope slides in Würzburg. *Philos. Trans. R. Soc. B Biol. Sci.* **369**, (2014). doi:10.1098/rstb.2013.0469

6. Fukasawa, K. *et al*. Abnormal centrosome amplification in the absence of p53. *Science (80-.).* **271**, 1744–1747 (1996). doi:10.1126/science.271.5256.1744

7. Bornens, M. The centrosome in cells and organisms. *Science (80-.).* **335**, 422–426 (2012). doi:10.1126/science.1209037

8. Gönczy, P. & Hatzopoulos, G. N. Centriole assembly at a glance. *J. Cell Sci.* **132**, (2019). doi:10.1242/jcs.228833

9. Bettencourt-Dias, M. & Glover, D. M. Centrosome biogenesis and function: Centrosomics brings new understanding. *Nat. Rev. Mol. Cell Biol.* **8**, 451–463 (2007). doi:10.1038/nrm2180

10. Vertii, A. *et al.* The centrosome, a multitalented renaissance organelle. *Cold Spring Harb. Perspect. Biol.* **8**, 1–14 (2016). doi:10.1101/cshperspect.a025049

11. Holland, A. J. *et al.* Centriole duplication: A lesson in self-control. *Cell Cycle* **9**, 2803–2808 (2010). doi:10.4161/cc.9.14.12184

12. Moyer, T. C. *et al.* Binding of STIL to Plk4 activates kinase activity to promote centriole assembly. *J. Cell Biol.* **209**, 863–878 (2015). doi:10.1083/jcb.201502088

13. Nakazawa, Y. *et al.* SAS-6 is a Cartwheel Protein that Establishes the 9-Fold Symmetry of the Centriole. *Curr. Biol.* **17**, 2169–2174 (2007). doi:10.1016/j.cub.2007.11.046

14. Ohta, M. *et al.* Direct interaction of Plk4 with STIL ensures formation of a single procentriole per parental centriole. *Nat. Commun.* **5**, 5267 (2014). doi:10.1038/ncomms6267

15. Chen, Z. *et al.* CP110, a cell cycle-dependent CDK substrate, regulates centrosome duplication in human cells. *Dev. Cell* **3**, 339–350 (2002). doi:10.1016/s1534-5807(02)00258-7

16. Schmidt, T. I. *et al.* Control of Centriole Length by CPAP and CP110. *Curr. Biol.* **19**, 1005–1011 (2009). doi:10.1016/j.cub.2009.05.016

17. Conduit, P. T. *et al.* Centrosome function and assembly in animal cells. *Nat. Rev. Mol. Cell Biol.* **16**, 611–624 (2015). doi:10.1038/nrm4062

18. Kong, D. *et al.* Centriole maturation requires regulated Plk1 activity during two consecutive cell cycles. *J. Cell Biol.* **206**, 855–865 (2014). doi:10.1083/jcb.201407087

19. Nigg, E. A. & Raff, J. W. Centrioles, Centrosomes, and Cilia in Health and Disease. *Cell* **139**, 663–678 (2009). doi:10.1016/j.cell.2009.10.036

20. Arquint, C. *et al.* Centrosomes as signalling centres. *Philos. Trans. R. Soc. B Biol. Sci.* **369**, (2014). doi:10.1098/rstb.2013.0464

21. Mullee, L. I. & Morrison, C. G. Centrosomes in the DNA damage response—the hub outside the centre. *Chromosom. Res.* **24**, 35–51 (2016). doi:10.1007/s10577-015-9503-7

22. Nigg, E. A. & Holland, A. J. Once and only once: Mechanisms of centriole duplication and their deregulation in diseases. *Nat. Rev. Mol. Cell Biol.* **19**, 297–312 (2018). doi:10.1038/nrm.2017.127

23. Chan, J. Y. Clinical Overview of Centrosome Amplification in Human Cancers. *Int. J. Biol. Sci.* **7**, 1122–1144 (2011). doi:10.7150/ijbs.7.1122

24. Nigg, E. A. Origins and consequences of centrosome aberrations in human cancers. *Int. J. Cancer* **119**, 2717–2723 (2006). doi:10.1002/ijc.22245

25. Levine, M. S. *et al.* Centrosome Amplification Is Sufficient to Promote Spontaneous Tumorigenesis in Mammals. *Dev. Cell* **40**, 313-322.e5 (2017). doi:10.1016/j.devcel.2016.12.022

26. Ganem, N. J. *et al.* A mechanism linking extra centrosomes to chromosomal instability. *Nature* **460**, 278–282 (2009). doi:10.1038/nature08136

27. Gönczy, P. Centrosomes and cancer: revisiting a long-standing relationship. *Nat. Publ. Gr.* **15**, 639–652 (2015). doi:10.1038/nrc3995

28. Mahjoub, M. R. The importance of a single primary cilium. *Organogenesis* **9**, 61–69 (2013). doi:10.4161/org.25144

29. Godinho, S. A. *et al.* Oncogene-like induction of cellular invasion from centrosome amplification. *Nature* **510**, 167–171 (2014). doi:10.1038/nature13277

30. Lomastro, G. M. & Holland, A. J. Perspective The Emerging Link between Centrosome Aberrations and Metastasis. *Dev. Cell* **49**, 325–331 (2019). doi:10.1016/j.devcel.2019.04.002

31. Bakir, B. *et al.* EMT , MET , Plasticity , and Tumor Metastasis. *Trends Cell Biol.* **30**, 764–776 (2020). doi:10.1016/j.tcb.2020.07.003

32. Chen, T. *et al.* Epithelial-mesenchymal transition (EMT): A biological process in the development, stem cell differentiation and tumorigenesis. *Journal of cellular physiology*, **232**, 3261-3272 (2017). doi:10.1002/jcp.25797

33. Pastushenko, I. & Blanpain, C. EMT Transition States during Tumor Progression and Metastasis. *Trends Cell Biol.* **29**, 212–226 (2019). doi:10.1016/j.tcb.2018.12.001

34. Loh, C. *et al.* The E-Cadherin and N-Cadherin Switch in Epithelial-to-Mesenchymal Transition: Signaling, Therapeutic Implications, and Challenges. *Cell* **8**, 1118 (2019). doi:10.3390/cells8101118

35. Kramer, N. *et al.* In vitro cell migration and invasion assays. *Mutat. Res. - Rev. Mutat. Res.* **752**, 10–24 (2013). doi:10.1016/j.mrrev.2012.08.001

36. Thiery, J. P. *et al.* Epithelial-Mesenchymal Transitions in Development and Disease. *Cell* 139, 871–890 (2009) doi:10.1016/j.cell.2009.11.007

37. Liao, Z. *et al.* High PLK4 expression promotes tumor progression and induces epithelial-mesenchymal transition by regulating the Wntβ-catenin signaling pathway in colorectal cancer. *International journal of oncology* **54**, 479-490 (2019). doi:10.3892/ijo.2018.4659

38. Tian, X. *et al.* Polo-like kinase 4 mediates epithelial – mesenchymal transition in neuroblastoma via PI3K / Akt signaling pathway. *Cell Death Dis.* **9**, 54 (2018) doi:10.1038/s41419-017-0088-2.

39. Garvey, D. *et al.* Role of Polo-Like Kinase 4 (PLK4) in Epithelial Cancers and Recent Progress in its Small Molecule Targeting for Cancer Management. *Molecular cancer therapeutics* **20**, 632-640 (2021). doi:10.1158/1535-7163.MCT-20-0741

40. Arnandis, T. *et al.* Oxidative Stress in Cells with Extra Centrosomes Drives Non-Cell-Autonomous Invasion. *Dev. Cell* **47**, 409-424.e9 (2018). doi:10.1016/j.devcel.2018.10.026

41. Ganier, O. *et al.* Structural centrosome aberrations sensitize polarized epithelia to basal cell extrusion. *Open biology* **8** (2018). doi:10.1098/rsob.180044

42. Reid, B. J. *et al.* Barrett's oesophagus and oesophageal adenocarcinoma: Time for a new synthesis. *Nat. Rev. Cancer* **10**, 87–101 (2010). doi:10.1038/nrc2773

43. Allison, P. R. & Johnstone, A. S. The oesophagus lined with gastric mucous membrane. *Thorax* **8**, 87–101 (1953). doi:10.1136/thx.8.2.87

44. McDonald, S. A. C. *et al.* Barrett oesophagus: Lessons on its origins from the lesion itself. *Nat. Rev. Gastroenterol. Hepatol.* **12**, 50–60 (2015). doi:10.1038/nrgastro.2014.181

45. Mukaisho, K. *et al.* Barretts's carcinogenesis. *Pathol. Int.* **69**, 319–330 (2019). doi:10.1111/pin.12804

46. Rhee, H. & Wang, D. H. Cellular Origins of Barrett's Esophagus: the Search Continues. *Curr. Gastroenterol. Rep.* **20**, 1–5 (2018). doi:10.1007/s11894-018-0657-2

47. Nowicki-Osuch, K. *et al.* Molecular phenotyping reveals the identity of Barrett's esophagus and its malignant transition. *Science (80-.).* **373**, 760–767 (2021). doi:10.1126/science.abd1449

48. Fitzgerald, R. C. *et al.* British Society of Gastroenterology guidelines on the diagnosis and management of Barrett's oesophagus. *Gut* **63**, 7–42 (2014). doi:10.1136/gutjnl-2013-305372

49. Lopes, C. A. M. *et al.* Centrosome amplification arises before neoplasia and increases upon p53 loss in tumorigenesis. *J. Cell Biol.* **217**, 2353–2363 (2018). doi:10.1083/jcb.201711191

50. Fléjou, J. F. Barrett's oesophagus: From metaplasia to dysplasia and cancer. *Gut* **54**, 6–13 (2005). doi:10.1136/gut.2004.041525

51. Schouten, L. J. *et al.* Total Cancer Incidence and Overall Mortality Are Not Increased Among Patients With Barrett's Esophagus. *Clin. Gastroenterol. Hepatol.* **9**, 754–761 (2011). doi:10.1016/j.cgh.2011.04.008

52. Bisschops, R. Barrett's esophagus: An exaggerated risk? *Ann. Gastroenterol.* **25**, 79–80 (2012).

53. Soussi, T. The p53 Tumor Suppressor Gene : From molecular biology to clinical investigation. *Annals of the New York Academy of Sciences* **910**, 121-37. (2000). doi:10.1111/j.1749-6632.2000.tb06705.x

54. Zhang, Q. *et al.* Acidic Bile Salts Induce Epithelial to Mesenchymal Transition via VEGF Signaling in Non-Neoplastic Barrett's Cells. *Gastroenterology* **156**, 130-144.e10 (2019). doi:10.1053/j.gastro.2018.09.046

55. Kazazian, K. *et al.* Plk4 Promotes Cancer Invasion and Metastasis through Arp2 / 3 Complex Regulation of the Actin Cytoskeleton. **1640**, 434-447 (2017). doi:10.1158/0008-5472.CAN-16-2060

56. Palanca-Wessels, M. C. A. *et al.* Extended lifespan of Barrett's esophagus epithelium transduced with the human telomerase catalytic subunit: A useful in vitro model. *Carcinogenesis* **24**, 1183–1190 (2003). doi:10.1093/carcin/bgg076

57. Wong, Y. L. *et al.* Reversible centriole depletion with an inhibitor of Polo-like kinase 4. *Science (80-.).* **348**, 1155–1160 (2015). doi:10.1126/science.aaa5111

58. Habedanck, R. *et al.* The Polo kinase Plk4 functions in centriole duplication. *Nat. Cell Biol.* **7**, 1140–1146 (2005). doi:10.1038/ncb1320

59. Oegema, K., Davis, R. L., Lara-Gonzalez, P., Desai, A. & Shiau, A. K. CFI-400945 is not a selective cellular PLK4 inhibitor. *Proc. Natl. Acad. Sci. U. S. A.* **115**, E10808–E10809 (2018). doi:10.1073/pnas.1813310115

60. Jaiswal, K. R. *et al.* Characterization of telomerase-immortalized, non-neoplastic, human Barrett's cell line (BAR-T). *Dis. Esophagus* **20**, 256–264 (2007). doi:10.1111/j.1442-2050.2007.00683.x

61. Kazazian, K. *et al.* Plk4 promotes cancer invasion and metastasis through Arp2/3 complex regulation of the actin cytoskeleton. *Cancer Res.* **77**, 434–447 (2017). doi:10.1158/0008-5472.CAN-16-2060

62. Kazazian, K. *et al.* Plk4 Promotes Cancer Invasion and Metastasis through Arp2 / 3 Complex Regulation of the Actin Cytoskeleton. **1640**, 1–15 (2016). doi:10.1158/0008-5472.CAN-16-2060

63. Rosario, C. O. *et al.* A novel role for Plk4 in regulating cell spreading and motility. *Oncogene* **34**, 3441–3451 (2015). doi:10.1038/onc.2014.275

64. Liu, Y. *et al.* Direct interaction between CEP85 and STIL mediates PLK4-driven directed cell migration. *J. Cell Sci.* **133**, (2020). doi:10.1242/jcs.238352

65. Mack, N. A. *et al.* The diverse roles of Rac signaling in tumorigenesis. *Cell Cycle* **10**, 1571–1581 (2011). doi:10.4161/cc.10.10.15612

66. Molinie, N. & Gautreau, A. The Arp2/3 regulatory system and its deregulation in cancer. *Physiol. Rev.* **98**, 215–238 (2018). doi:10.1152/physrev.00006.2017

67. Zheng, H. C. *et al.* Arp2/3 overexpression contributed to pathogenesis, growth and invasion of gastric carcinoma. *Anticancer Res.* **28**, 2225–2232 (2008).

68. Chaffer, C. L. *et al.* EMT , cell plasticity and metastasis. *Cancer Metastasis Rev.* (2016) doi:10.1007/s10555-016-9648-7. doi:10.1007/s10555-016-9648-7

69. Lin, T. C. *et al.* Fibronectin in Cancer: Friend or Foe. *Cells* **9**, 1–37 (2019). doi:10.3390/cells9010027

70. Sung, B. H. *et al.* Directional cell movement through tissues is controlled by exosome secretion. *Nat. Commun.* **6**, (2015). doi:10.1038/ncomms8164

71. Xiong, G.-F. & Xu, R. Function of cancer cell-derived extracellular matrix in tumor progression. *J. Cancer Metastasis Treat.* **2**, 357 (2016).

72. Armstrong, H. K. *et al.* Dysregulated fibronectin trafficking by Hsp90 inhibition restricts prostate cancer cell invasion. Sci. Rep. 8, 1–14 (2018). doi:10.1038/s41598-018-19871-4

73. Hehnly, H. et al. The centrosome regulates the Rab11- dependent recycling endosome pathway at appendages of the mother centriole. Curr. Biol. 22, 1944–1950 (2012). doi:10.1016/j.cub.2012.08.022

7. SUPPLEMENTARY FIGURES

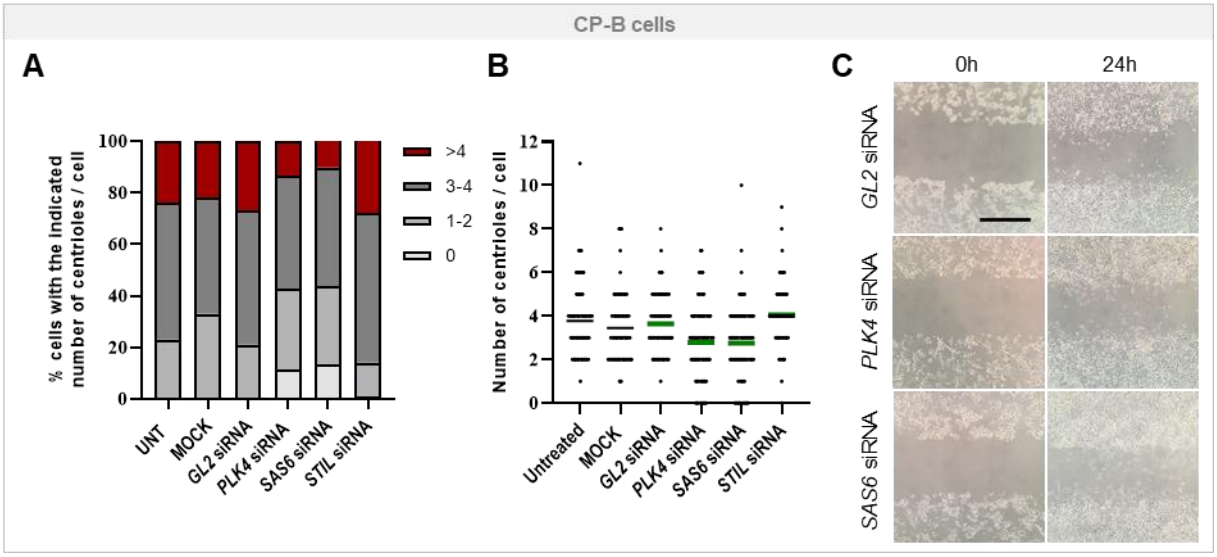

Figure S7.1 (Related to Figure 3.2) – Migration and invasion assays with CP-B cells with reduced CA by depleting core centriole protein by siRNA. Dysplasia CP-B cells transfected with control (*GL2*) or *PLK4*, *SAS6* and *STIL* siRNA for 3 days were submitted to migration and invasion assays (wound healing and transwell migration and invasion assays). **(A)** Quantification of interphase cells with the indicated number of centrioles in each cell. **(B)** Number of centrioles in each cell. Green line indicates mean. (N=1; n=100 cells/condition). **(C)** Bright-field microscopy images of wound closure at time zero (0h) and 24h after creating wound/gap. Scale bar: 0.5mm.

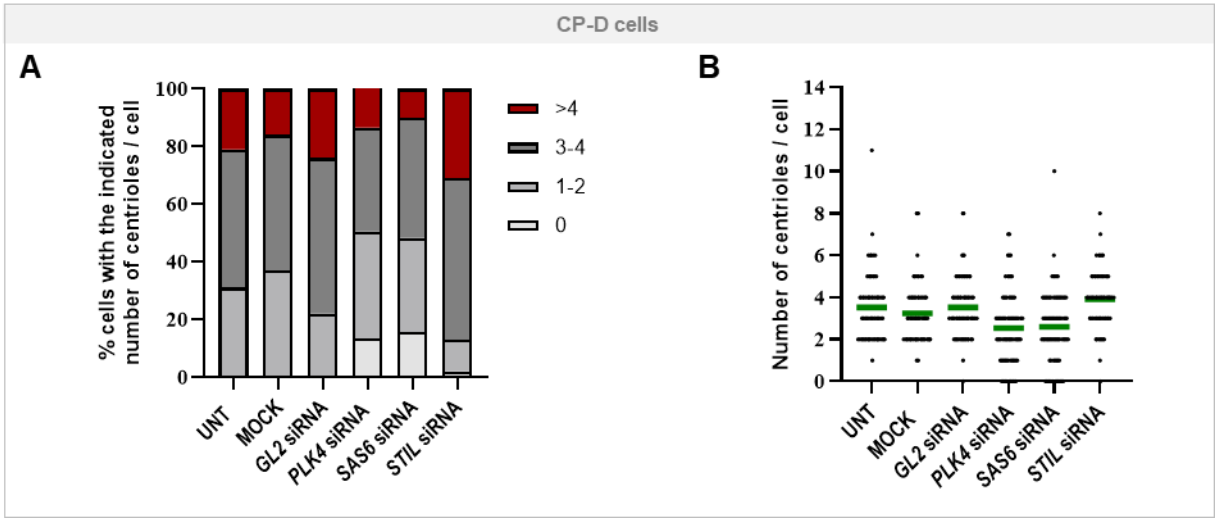

Figure S7.2 (Related to Figure 3.3) – – Migration and invasion assays with CP-D cells with reduced CA by depleting core centriole protein by siRNA. Dysplasia CP-D cells transfected with control (*GL2*) or *PLK4*, *SAS6* and *STIL* siRNA for 3 days were submitted to migration and invasion assays (wound healing and transwell migration and invasion assays). **(A)** Quantification of interphase cells with the indicated number of centrioles in each cell. **(B)** Number of centrioles in each cell. Green line indicates mean. (N=1; n=100 cells/condition).

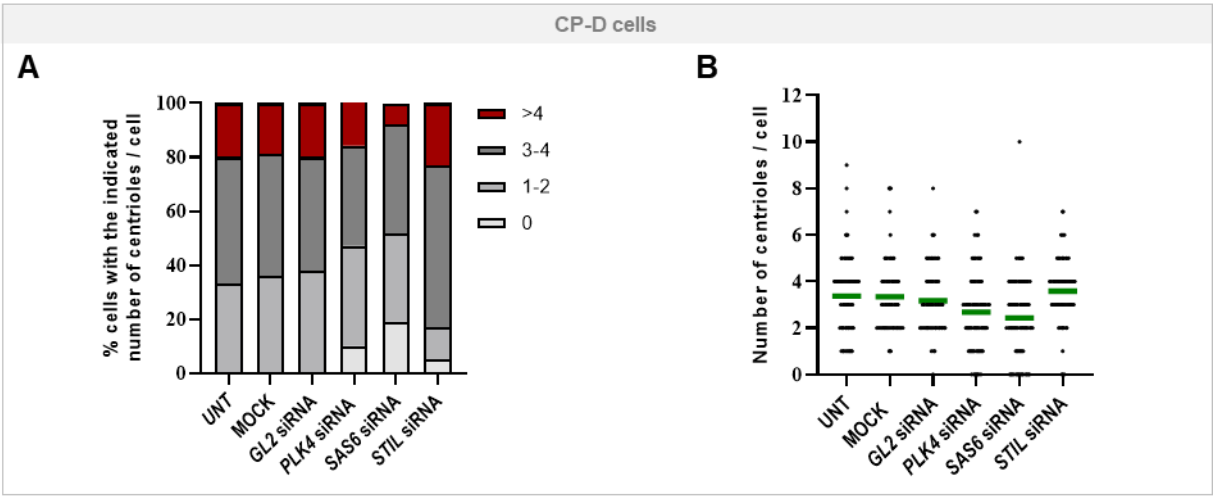

Figure S7.3 (Related to Figure 3.4) – Optimized migration and invasion assays with CP-D cells with reduced CA by depletion of core centriole biogenesis proteins by siRNA. Dysplasia CP-D cells transfected with control (*GL2*) or *PLK4*, *SAS6* and *STIL* siRNA for 3 days were submitted to migration and invasion assays (wound healing and transwell migration and invasion assays). **(A)** Quantification of interphase cells with the indicated number of centrioles in each cell. **(B)** Number of centrioles in each cell. Green line indicates mean. (N=1; n=100 cells/condition).

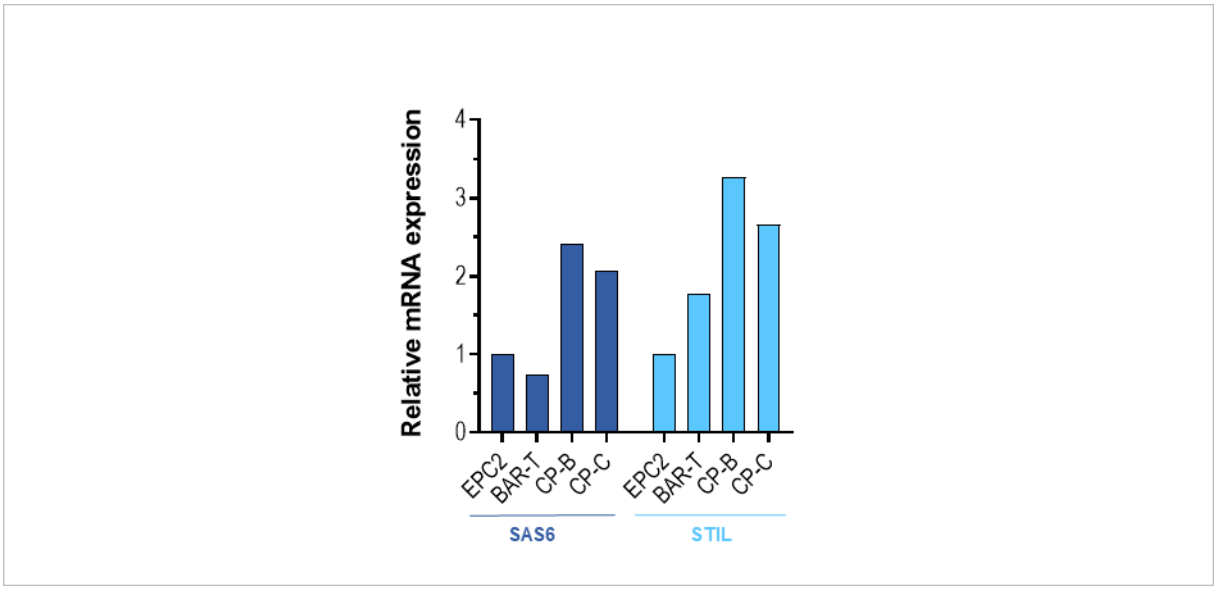

Figure S7.4 – qRT–PCR showing the relative mRNA expression of SAS6 and STIL throughout BE progression.

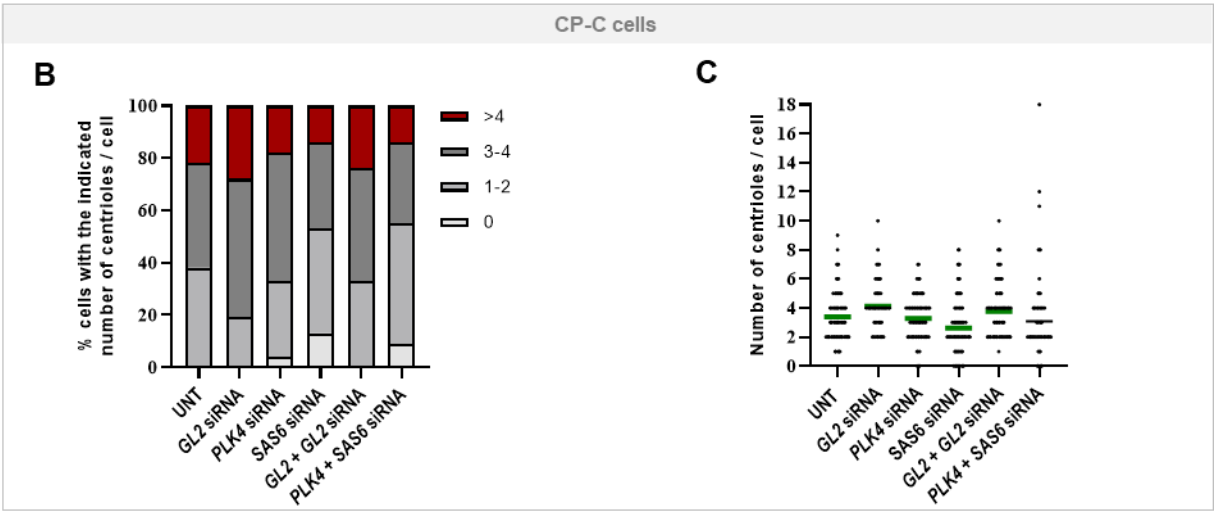

Figure S7.5 (Related to Figure 3.5) - Dysplasia cells with reduced CA through depletion of core centriole biogenesis proteins by siRNA showed a reduced invasiveness capacity in 3D cultures. Dysplasia CP-C cells transfected with control (*GL2*) or *PLK4*, *SAS6* siRNA and *PLK4+SAS6* co-depletion siRNA were grown in 3D cell cultures to assess for invasion. **(A)** Quantification of interphase cells with the indicated number of centrioles in each cell. **(B)** Number of centrioles in each cell. Green line indicates mean. (N=1; n=100 cells/condition).

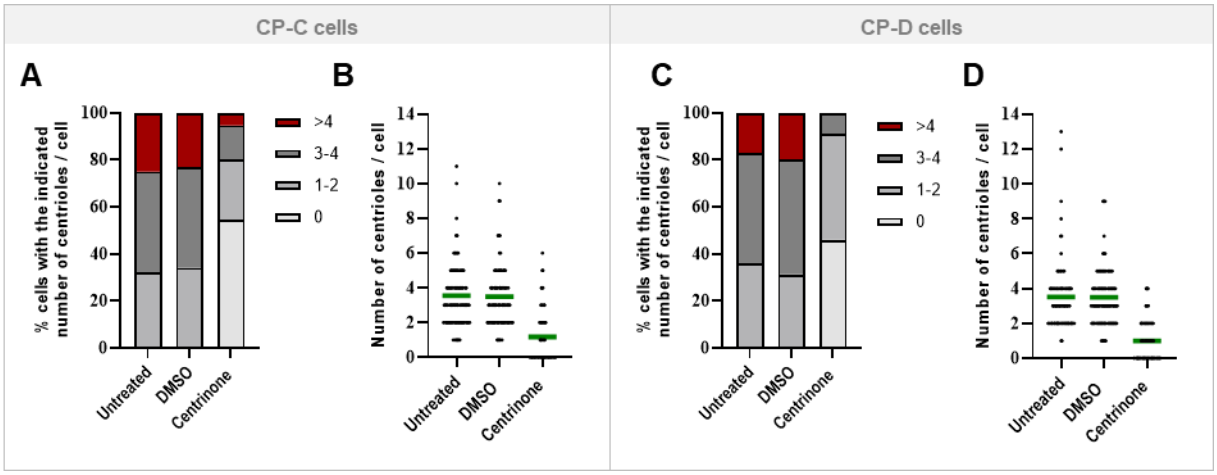

Figure S7.6 (Related to Figure 3.9) – Migration and invasion assays in dysplasia cells with reduced CA through PLK4 inhibition by centrinone. CP-C (A-B) and CP-D (C-D) dysplasia cells treated with centrinone were submitted to 2D migration and invasion assays (wound healing and transwell invasion assays). **(A and C)** Quantification of interphase cells with the indicated number of centrioles in each cell. **(B and D)** Number of centrioles in each cell. Green line indicates mean. (N=1; n=100 cells/condition).

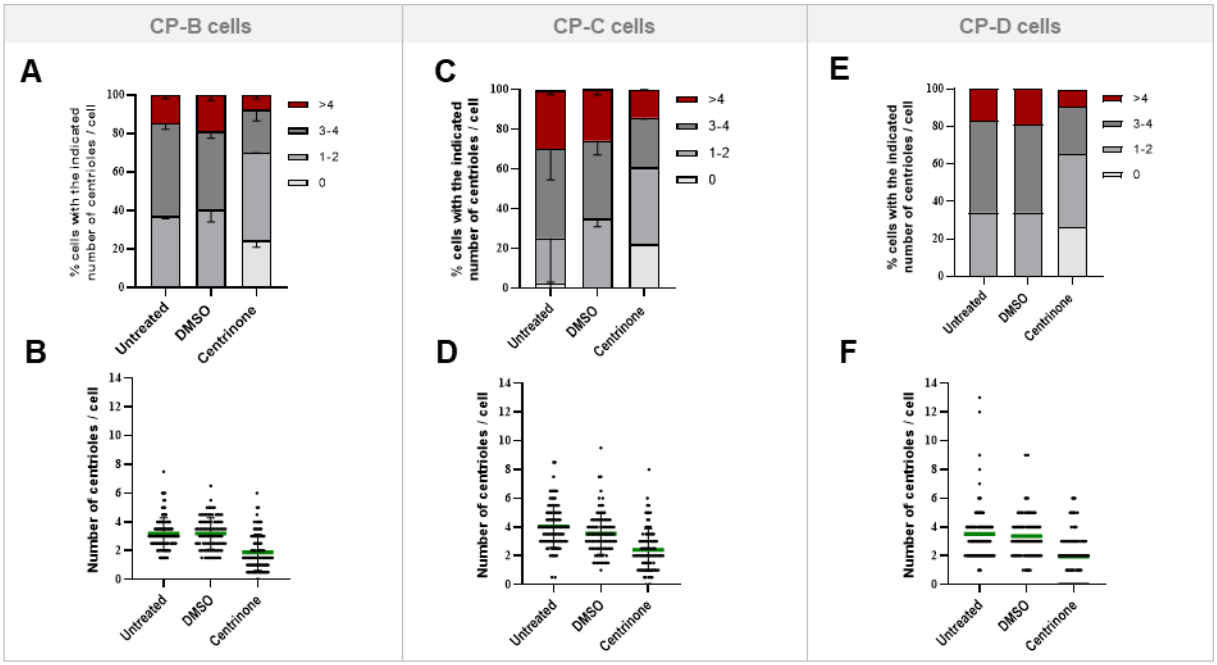

Figure S7.7 (Related to Figure 3.10) – Dysplasia cells used for 3D cell cultures showed a reduction of CA through PLK4 inhibition by centrinone. CP-B (B), CP-C (C) and CP-D (D) dysplasia cells treated with centrinone were grown in 3D cultures. **(A, C and E)** Quantification of interphase cells with the indicated number of centrioles in each cell. (A and C) N=2; n=100 cells/condition. Mean ± standard deviation. (E) N=1; n=100 cells/condition. **(B, D and F)** Number of centrioles in each cell. Green line indicates mean. (B and D) N=2; n=100 cells/condition. Mean ± standard deviation. (F) N=1; n=100 cells/condition.

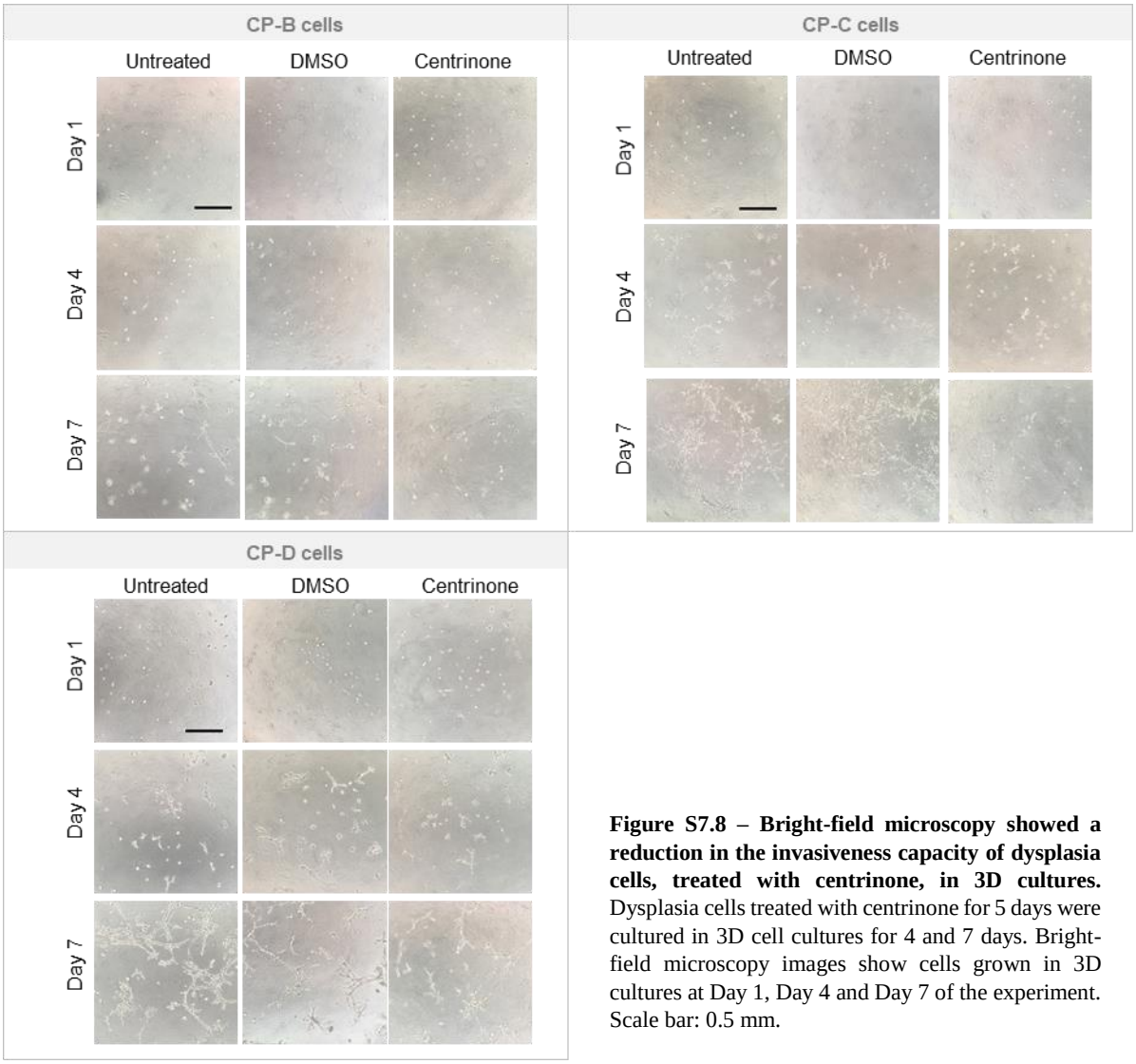

Figure S7.8 – Bright-field microscopy showed a reduction in the invasiveness capacity of dysplasia cells, treated with centrinone, in 3D cultures. Dysplasia cells treated with centrinone for 5 days were cultured in 3D cell cultures for 4 and 7 days. Bright-field microscopy images show cells grown in 3D cultures at Day 1, Day 4 and Day 7 of the experiment. Scale bar: 0.5 mm.

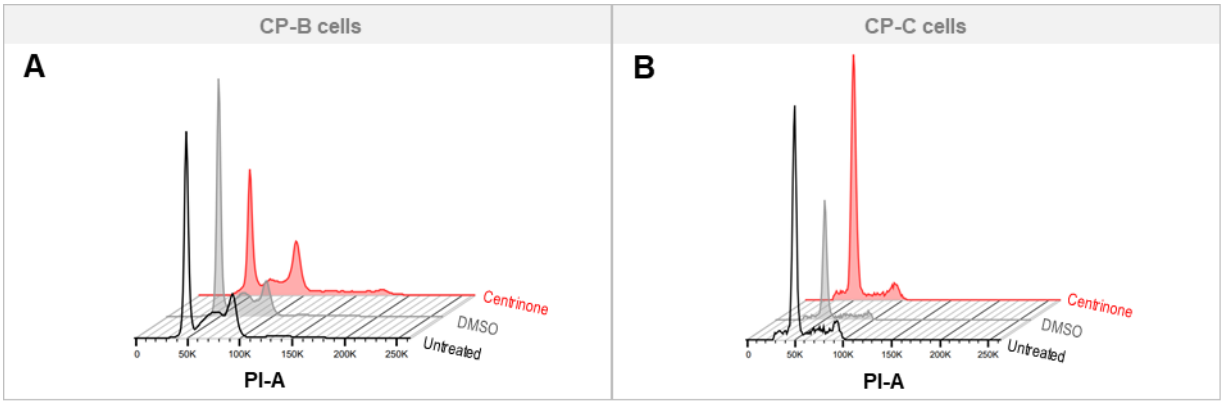

Figure S7.9 (Related to Figures 3.10 and 3.11) – Inhibition of PLK4, by centrinone, increased ploidy in dysplasia cells. CP-B, and CP-C dysplasia cells treated with centrinone-B for 5 days were cultured in 3D cell cultures.**(A)** Flow cytometry analysis performed in CP-B cells after 12 days of centrinone treatment (Day 7 of 3D cultures). Untreated: 8788 cells; DMSO: 8724 cells; Centrinone: 8236 cells **(B).** Flow cytometry analysis performed in CP-C cells after 12 days of centrinone treatment (Day 0 of 3D cultures). Untreated: 7778 cells; DMSO: 4041 cells; Centrinone: 8768.

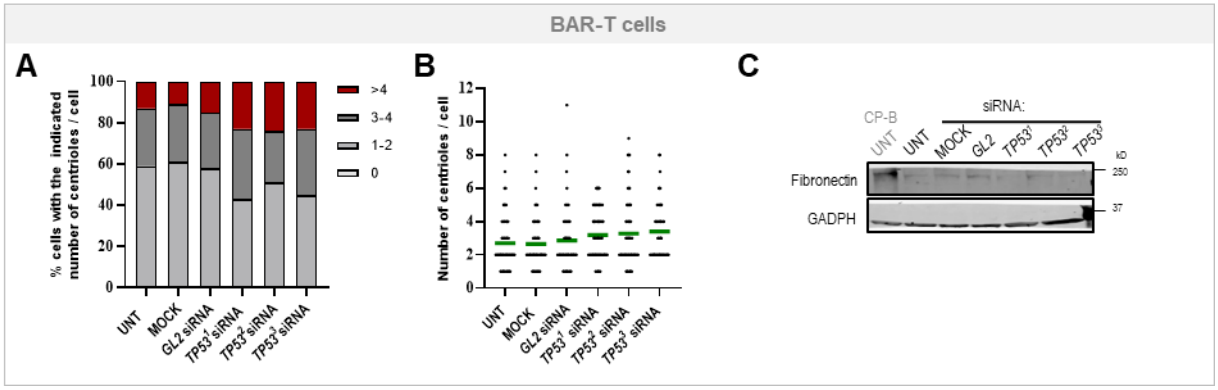

Figure S7.10 (Related to Figure 3.12) – Metaplasia cells with increased CA did not show differences in the invasiveness capacity in 3D cultures. BAR-T metaplasia cells transfected with control (*GL2)* or *TP53* siRNA were grown in 3D cultures. **(A)** Quantification of interphase cells with the indicated number of centrioles in each cell. **(B)** Number of centrioles in each cell. Green line indicates mean. (N=1; n=100 cells/condition). (C) Protein levels assessed by western blot. CP-B dysplasia cells were used as a positive control.